

# Shallow neural network yields regularization for ill-posed inverse problems

Lan Wang, Qiao Zhu, Bangti Jin, and Ye Zhang

## Abstract

In this paper, we establish universal approximation theorems for neural networks applied to general nonlinear ill-posed operator equations. In addition to the approximation error, the measurement error is also taken into account in our error estimation. We introduce the expanding neural network method as a novel iterative regularization scheme and prove its regularization properties under different a priori assumptions about the exact solutions. Within this framework, the number of neurons serves as both the regularization parameter and iteration number. We demonstrate that for data with high noise levels, a small network architecture is sufficient to obtain a stable solution, whereas a larger architecture may compromise stability due to overfitting. Furthermore, under standard assumptions in regularization theory, we derive convergence rate results for neural networks in the context of variational regularization. Several numerical examples are presented to illustrate the robustness of the proposed neural network-based algorithms.

## Index Terms

Ill-posed inverse problems, two layer networks, universal approximation theorems, iterative regularization, Tikhonov regularization, convergence rates

## I. INTRODUCTION

**I**NVERSE problems arise in various scientific and engineering fields, including medical imaging, geophysics, and computational physics. These problems often involve reconstructing unknown parameters or functions from indirect, noisy, and sometimes incomplete measurements. Traditional approaches rely on regularization techniques, optimization algorithms, and statistical inference. However, these methods often suffer from computational inefficiency, sensitivity to noise, and the need for handcrafted priors. With the rapid advancement of deep learning, neural networks have emerged as powerful tools for solving inverse problems. Their ability to learn complex mappings from data has significantly improved reconstruction accuracy and computational efficiency. In this paper, we study the neural network methods for solving general operator equations

$$A(f) = g, \quad (1)$$

where  $A \in \mathbb{M}(\mathcal{X}, \mathcal{Y})$ , and  $\mathbb{M}(\mathcal{X}, \mathcal{Y})$  denotes the space of all bounded (possibly non-linear) operators between two reflexive Banach spaces of functions. For simplicity, we denote by  $\|\cdot\|$  the norms for both Banach spaces. The precise setting of ambient spaces for functions  $f$  and  $g$  will be proposed later in Section II. Suppose that instead of inexact right-hand side  $g$ , we are given only perturbed element  $g^\delta$ , obeying the deterministic noise model with noise level  $\delta > 0$ :

$$\|g^\delta - g\|_{\mathcal{Y}} \leq \delta. \quad (2)$$

**Definition 1.** [1] A mapping  $\mathcal{R} : \mathbb{M}(\mathcal{X}, \mathcal{Y}) \times \mathcal{Y} \times \mathbb{R}_+ \rightarrow \mathcal{X}$  is called a regularization method of inverse problems (1)-(2) if the following two conditions are satisfied:

- 1) brings  $f^\delta = \mathcal{R}(A, g^\delta, \delta) \in \mathcal{X}$  into correspondence with any data  $\{g^\delta, \delta\}$  of (1).
- 2) has the convergence property (in some topology):

$$f^\delta \rightarrow f^\dagger \text{ as } \delta \rightarrow 0. \quad (3)$$

The element  $f^\delta$ , satisfying the above two conditions, is called a regularization solution of inverse problems (1)-(2).

The computational inverse problem for solving operator equations is formulated as follows:

**(IP):** Given inexact data  $g^\delta$  with the noise model (2) and the forward model (1), find a regularization solution  $f^\delta$  of inverse problems (1)-(2).

According to Tikhonov's definition of regularization – Definition 1, if a regularization solution, says  $f^\delta$ , exists for **(IP)**, there must exist infinite number of regularization solutions, e.g.  $f^\delta + h(\delta)$  with any vanishing function  $h$  (i.e.  $h(\delta) \rightarrow 0$  as  $\delta \rightarrow 0$ ) can be severed as another regularization solution according to the definition of regularization solution (3). The main goal in

L. Wang, Q. Zhu and Y. Zhang are with the School of Mathematics and Statistics, Beijing Institute of Technology, Beijing 100081, China.

B. Jin is with the Department of Mathematics, The Chinese University of Hong Kong, Shatin, N.T., Hong Kong.

Y. Zhang is also with the MSU-BIT-SMBU Joint Research Center of Applied Mathematics, Shenzhen MSU-BIT University, Shenzhen 518172, China.

Corresponding author: Y. Zhang (e-mail: ye.zhang@smbu.edu.cn).

This work was supported by the Shenzhen Sci-Tech Fund (No. RCJC20231211090030059) and National Natural Science Foundation of China (No. 12171036).

this work is answer if  $f^\delta$  can be a neural network, i.e. we aim to answer the following questions, which will be referred as *the universal approximation theory of neural networks for inverse problems*:

- (Q1): Does there exist a neural network  $\mathcal{NN}$  that provides a regularized solution to (1) in the presence of noisy data?
- (Q2): Is a larger neural network always preferable for solving ill-posed inverse problems with noisy data, or is there a fundamental limitation on the size or complexity of  $\mathcal{NN}$ ? What's the relation between noise level and size of neural network?
- (Q3): If such a limitation exists, how can one construct a neural network  $\mathcal{NN}$  with minimal architectural complexity that remains effective in solving the inverse problem with noisy data?
- (Q4): What is the optimal size of a neural network for a regularization method based on neural networks that achieves optimal convergence rates with respect to the noise level for general non-linear ill-posed problems (1)?

The traditional universal approximation theory characterizes the ability of neural networks to approximate arbitrary functions under certain conditions. Foundational results were established for shallow (single-hidden-layer) neural networks, demonstrating that a single hidden layer suffices for universal approximation, notably by Cybenko (1989) [2], Hornik (1989, 1991) [3], [4], and Stinchcombe & White (1989) [5], followed by Barron (1993) [6], who further quantified approximation rates. Subsequent research shifted the focus to deeper architectures, leading to significant advancements. It was demonstrated that deep networks with moderate width can approximate certain functions exponentially more efficiently than shallow networks with large width, as shown by Telgarsky (2016) [7] and Eldan & Shamir (2016) [8]. Table I provides a summary of existing approximation error bounds for fully connected feedforward neural networks (FNNs) with ReLU activation functions.

TABLE I  
A SUMMARY OF EXISTING APPROXIMATION ERRORS OF RELU FNNs. HERE,  $d, s \in \mathbb{N}^+$  AND HÖLDER( $[0, 1]^d, \alpha$ ) DENOTES THE SPACE OF HÖLDER CONTINUOUS FUNCTIONS OF ORDER  $\alpha \in (0, 1]$ .

Reference	Function class	Width ( $n$ )	Depth ( $l$ )	Approximation error	Norm
[9]	polynomial	$\mathcal{O}(n)$	$\mathcal{O}(l)$	$\mathcal{O}(n^{-l})$	$L^\infty([0, 1]^d)$
[10]	Hölder( $[0, 1]^d, \alpha$ )	$\mathcal{O}(n)$	$\mathcal{O}(l)$	$\mathcal{O}((n^2 l^2 \ln n)^{-\alpha/d})$	$L^p([0, 1]^d), p \in [1, \infty]$
[11]	$C([0, 1]^d)$	$\mathcal{O}(n)$	$\mathcal{O}(l)$	$\mathcal{O}(n^{-2/d} l^{-2/d})$	$L^p([0, 1]^d), p \in [1, \infty]$
[10], [12]	$C([0, 1]^d)$	$\mathcal{O}(n)$	$\mathcal{O}(l)$	$\mathcal{O}((n^2 l^2 \ln n)^{-1/d})$	$L^p([0, 1]^d), p \in [1, \infty]$
[13]	$C([0, 1]^d)$	$\max\{d+1, 5\}$	$\mathcal{O}(l)$	$\mathcal{O}(l^{-2/d})$	$L^p([0, 1]^d), p \in [1, \infty]$
[14]	$C^s([0, 1]^d)$	$2d+10$	$\mathcal{O}(l)$	$\mathcal{O}((l/\ln l)^{-2s/d})$	$L^\infty([0, 1]^d)$
[9], [12]	$C^s([0, 1]^d)$	$\mathcal{O}(n \ln n)$	$\mathcal{O}(l \ln l)$	$\mathcal{O}(n^{-2s/d} l^{-2s/d})$	$L^\infty([0, 1]^d)$
[9]	$C^s([0, 1]^d)$	$\mathcal{O}(n)$	$\mathcal{O}(l)$	$\mathcal{O}((n/\ln n)^{-2s/d} (l/\ln l)^{-2s/d})$	$L^\infty([0, 1]^d)$
[15]	$C^s([0, 1]^d), s > 1$	$\mathcal{O}(n \log n)$	$\mathcal{O}(l \log l)$	$\mathcal{O}(n^{-2(s-1)/d} l^{-2(s-1)/d})$	$\mathcal{W}^{1,p}([0, 1]^d), p \in [1, \infty]$

With the development of the universal approximation theory and the ability of neural networks to model complex nonlinear relationships, neural networks have emerged as powerful tools for solving inverse problems. Current research applying neural networks to inverse problems can be broadly categorized into two main areas: parameter estimation and image reconstruction. For parameter estimation problems, particularly those governed by partial differential equations (PDEs), neural network-based approaches have exhibited superior effectiveness. In contrast with the traditional numerical approaches, neural network methods can efficiently handle high-dimensional parameter spaces, reduced computational complexity for complex systems, and enhanced performance with limited or noisy data. Over the past few years, numerous neural network-based models have been proposed and applied to solve PDEs, addressing both forward and inverse problems. Deep Ritz Method (DRM) [16] reformulates PDEs as variational problems to leverage neural networks' approximation capabilities. Deep Galerkin Method (DGM) [17] efficiently solves high-dimensional PDEs by using Monte Carlo approximation to replace second-order derivatives. Physics-informed neural networks (PINN) [18] embed physical laws into the training process, enabling physically consistent predictions with less reliance on large datasets. Weak Adversarial Networks (WAN) [19] leverage adversarial training for solving PDEs in weak form. Generative Adversarial Networks (GAN) [20] generate realistic data samples by training two neural networks (generator and discriminator) in a competitive setting. Kolmogorov-Arnold Networks (KAN) [21] enhance interpretability by using explicit functional representations based on the Kolmogorov-Arnold theorem, while also maintaining high accuracy in complex tasks. These models have been successfully applied to parameter estimation tasks in various equations [22]–[27]. Convolutional Neural Networks (CNN) [28] and their variants, such as U-Net [29], have demonstrated remarkable success for image reconstruction problems. In Electrical Impedance Tomography (EIT), CNN effectively handles highly nonlinear and ill-posed inverse processes [30]–[32]. In Computed Tomography (CT), neural network methods enhance image quality and reduce artifacts under low-dose conditions [33]–[36]. In Magnetic Resonance Imaging (MRI), compressed sensing techniques combined with neural network methods enable fast and high-quality image reconstruction from undersampled data, significantly reducing scan times [37]–[39].

In this paper, inspired by iterative regularization methods [40], [41] and the method of extending compacts [42]–[44], we propose two expanding neural network methods based on prior knowledge of the energy upper bound of exact solutions. In these methods, the iteration number, which determines the neural network size, acts as the regularization parameter. Both the

iteration number and the neural network size are selected according to the a posteriori selection criterion—specifically, the Morozov discrepancy principle.

Furthermore, leveraging Tikhonov variational regularization theory, we establish a comprehensive regularization framework for shallow neural networks aimed at solving general inverse problems. To clearly illustrate our core concepts, we focus specifically on two-layer neural networks, which are relatively simple to construct and analyze. These two-layer networks serve as regularized solutions, approximating exact solutions to ill-posed problems. The appropriate functional space for analyzing two-layer networks is the so-called ‘‘Barron space’’, since functions in this space can be efficiently approximated by two-layer neural networks, as detailed in our subsequent analysis.

The remainder of the paper is structured as follows: Section II provides preliminary results regarding the properties of Barron spaces, forming the foundation for our analysis. Section III addresses iterative regularization, where we introduce the two proposed expanding neural network methods. In Section IV, we examine Tikhonov regularization and present convergence analyses, including convergence rates under variational source conditions. Numerical experiments demonstrating the effectiveness of our methods are presented in Section V, followed by concluding remarks in Section VI.

## II. SOME PROPERTIES OF BARRON SPACES

The functions defined in Barron space take the following representation

$$f(\mathbf{x}) = \int_P a\sigma(\mathbf{b}^T \mathbf{x} + c) \rho(da, d\mathbf{b}, dc), \quad \mathbf{x} \in \Omega \subset \mathbb{R}^d, \quad (4)$$

where  $P = \mathbb{R} \times \mathbb{R}^d \times \mathbb{R}$ ,  $\rho$  is a probability distribution on  $(P, \Sigma_P)$  with  $\Sigma_P$  being a Borel  $\sigma$ -algebra on  $P$ ,  $\sigma$  is activation function,  $\Omega$  is a bounded domain. In this paper we focus on the RELU activation function  $\sigma(z) := \max(0, z) := (z)_+$ .

For functions that admit the representation (4), we define a value with a given probability distribution  $\rho$ :

$$\|f\|_{\mathcal{B}_{p,\rho}} = (\mathbb{E}_\rho [|a|^p (\|\mathbf{b}\|_1 + |c|)^p])^{1/p} = \left( \int_P |a|^p (\|\mathbf{b}\|_1 + |c|)^p \rho(da, d\mathbf{b}, dc) \right)^{\frac{1}{p}}, \quad 1 \leq p \leq +\infty.$$

Then, the Barron norm of a function, having the structure (4), is defined as

$$\|f\|_{\mathcal{B}_p} = \inf_\rho \|f\|_{\mathcal{B}_{p,\rho}}. \quad (5)$$

With the above preparation, the Barron spaces  $\mathcal{B}_p$  are defined as the set of continuous functions that can be represented by (4) with finite Barron norm, i.e.

$$\mathcal{B}_p := \{f : f \text{ satisfies (4) and } \|f\|_{\mathcal{B}_p} < \infty\}. \quad (6)$$

**Proposition 1.** ([45]) *For any  $1 \leq p \leq \infty$ , we have  $\mathcal{B}_1 = \mathcal{B}_p$  (as sets) and  $\|f\|_{\mathcal{B}_1} = \|f\|_{\mathcal{B}_p}$ .*

**Proposition 2** (Properties of Barron space  $\mathcal{B}_1$ ). [46] (1) *The set  $\mathcal{B}_1$  equipped with the functional  $f \mapsto \|f\|_{\mathcal{B}_1}$  is a normed space.*

(2) *The Barron space  $\mathcal{B}_1$  is a subspace of standard Sobolev space  $H^1(\Omega)$ , and there exists a constant  $C(\Omega, d)$  such that for all  $f \in \mathcal{B}_1$  there holds  $\|f\|_{H^1(\Omega)} \leq C(\Omega, d)\|f\|_{\mathcal{B}_1}$ .*

Based on the favorable properties of the Barron space  $\mathcal{B}_1$ , we primarily focus on this function space in our subsequent analysis.

The approximation functions considered in this paper are the two-layer neural networks, which can be seen as the empirical analog of (4), have this representation

$$f_n = \frac{1}{n} \sum_{j=1}^n a_j \left( \mathbf{b}_j^T \mathbf{x} + c_j \right)_+, \quad (a_j, \mathbf{b}_j, c_j) \in \mathbb{R} \times \mathbb{R}^d \times \mathbb{R}. \quad (7)$$

To be mentioned here, it allows for a representation of (4), since it can be rewritten as

$$f_n(\mathbf{x}) = \int_P a \left( \mathbf{b}^T \mathbf{x} + c \right)_+ \rho_n(da, d\mathbf{b}, dc), \quad \mathbf{x} \in \Omega, \quad (8)$$

where  $\rho_n$  is a uniform probability on the point set  $(a_j, \mathbf{b}_j, c_j)_{j=1}^n$ .

Let  $r := r(n)$  be a monotonic increasing function, and define a  $r$ -bounded set of parameters:  $M_r := \{(a_j, \mathbf{b}_j, c_j) \in \mathbb{R} \times \mathbb{R}^d \times \mathbb{R}, |a_j| \leq r(n), \|\mathbf{b}_j\|_1 + |c_j| = 1\}$ . Obviously,  $M_r$  is a compact set in  $\mathbb{R} \times \mathbb{R}^d \times \mathbb{R}$ . Now, let us define the set of approximation functions of order  $n$ :

$$X_{n,r} := \left\{ f_n : f_n = \frac{1}{n} \sum_{j=1}^n a_j \left( \mathbf{b}_j^T \mathbf{x} + c_j \right)_+, (a_j, \mathbf{b}_j, c_j) \in M_r \right\}. \quad (9)$$

**Lemma 1.** Let  $\Omega$  be a bounded domain,  $K := \overline{\Omega}$ . Then, for any fixed  $n > 0$ ,  $X_{n,r}$  is sequentially compact in  $C(K)$  and  $L^2(\Omega)$ .

*Proof.* To establish the sequential compactness of  $X_{n,r(n)}$ , it suffices to verify that, for every sequence

$\left\{f_n(a^k, \mathbf{b}^k, c^k, \mathbf{x})\right\}_{k=1}^{+\infty} \subset X_{n,r(n)}$ , there exists a convergent subsequence whose limit lies in  $X_{n,r(n)}$ .

Due to the compactness of  $M_r$ , for any sequence  $\{(a^k, \mathbf{b}^k, c^k)\}_{k=1}^{\infty} \subset M_r$ , there exists a subsequence  $(a^{k_\ell}, \mathbf{b}^{k_\ell}, c^{k_\ell})$  and a pair  $(\tilde{a}, \tilde{\mathbf{b}}, \tilde{c}) \in M_r$  such that

$$(a^{k_\ell}, \mathbf{b}^{k_\ell}, c^{k_\ell}) \rightarrow (\tilde{a}, \tilde{\mathbf{b}}, \tilde{c}) \quad \text{as } \ell \rightarrow \infty, \quad \text{in } (\mathbb{R} \times \mathbb{R}^d \times \mathbb{R})^n.$$

Since  $K$  is bounded, there is  $R > 0$  with  $K \subset \{x : \|x\|_\infty \leq R\}$ . Write  $C_R := \max\{R, 1\}$ . Using that  $t \mapsto t_+$  is 1-Lipschitz and  $\|\mathbf{b}\|_1 + |c| = 1$ , for every  $x \in K$  we have

$$\begin{aligned} & |f_n(a^{k_\ell}, \mathbf{b}^{k_\ell}, c^{k_\ell}; \mathbf{x}) - f_n(\tilde{a}, \tilde{\mathbf{b}}, \tilde{c}; \mathbf{x})| \\ & \leq \frac{1}{n} \sum_{j=1}^n |a_j^{(k_\ell)} - \tilde{a}_j| |((\mathbf{b}_j^{(k_\ell)})^T \mathbf{x} + c_j^{(k_\ell)})_+| + \frac{1}{n} \sum_{j=1}^n |\tilde{a}_j| |((\mathbf{b}_j^{(k_\ell)})^T \mathbf{x} + c_j^{(k_\ell)})_+ - (\tilde{\mathbf{b}}_j^T \mathbf{x} + \tilde{c}_j)_+| \\ & \leq \frac{1}{n} \sum_{j=1}^n |a_j^{(k_\ell)} - \tilde{a}_j| (|(\mathbf{b}_j^{(k_\ell)})^T \mathbf{x}| + |c_j^{(k_\ell)}|) + \frac{1}{n} \sum_{j=1}^n |\tilde{a}_j| (|(\mathbf{b}_j^{(k_\ell)} - \tilde{\mathbf{b}}_j)^T \mathbf{x}| + |c_j^{(k_\ell)} - \tilde{c}_j|) \\ & \leq C_R \left[ \frac{1}{n} \sum_{j=1}^n |a_j^{(k_\ell)} - \tilde{a}_j| + \frac{1}{n} \sum_{j=1}^n |\tilde{a}_j| (\|\mathbf{b}_j^{(k_\ell)} - \tilde{\mathbf{b}}_j\|_1 + |c_j^{(k_\ell)} - \tilde{c}_j|) \right], \end{aligned}$$

Hence  $\|f_n(a^{k_\ell}, \mathbf{b}^{k_\ell}, c^{k_\ell}; \mathbf{x}) - f_n(\tilde{a}, \tilde{\mathbf{b}}, \tilde{c}; \mathbf{x})\|_{C(K)} \rightarrow 0$ , which means  $f_n(a^{k_\ell}, \mathbf{b}^{k_\ell}, c^{k_\ell}; \mathbf{x}) \rightarrow f_n(\tilde{a}, \tilde{\mathbf{b}}, \tilde{c}; \mathbf{x})$  in  $C(K)$ , proving sequential compactness. Moreover, we note that  $f_n(\tilde{a}, \tilde{\mathbf{b}}, \tilde{c}; \mathbf{x}) \in \mathcal{B}_1$  for the reason that  $\frac{1}{n} \sum_{j=1}^n |\tilde{a}_j| (\|\tilde{\mathbf{b}}_j\|_1 + |\tilde{c}_j|) = \frac{1}{n} \sum_{j=1}^n |\tilde{a}_j| \leq r(n) < +\infty$ .

Since  $\Omega$  is bounded, the natural map  $C(K) \rightarrow L^2(\Omega)$  is continuous with  $\|f\|_{L^2(\Omega)} \leq |\Omega|^{1/2} \|f\|_{C(K)}$ . Hence  $X_{n,r(n)}$  is also sequentially compact in  $L^2(\Omega)$ .  $\square$

**Lemma 2.** Any bounded sequence in Barron space  $\mathcal{B}_1$  has a subsequence that converges in  $H^1(\Omega)$ , and any bounded sequence in Barron space  $H^1(\Omega)$  has a subsequence that converges in  $L^2(\Omega)$ .

*Proof.* It follows from the fact that  $\mathcal{B}_1$  is continuously embedded into  $H^1(\Omega)$ , and  $H^1(\Omega)$  is compactly embedded into  $L^2(\Omega)$ .  $\square$

The following proposition shows that functions defined in the Barron space  $\mathcal{B}_1$  can be approximated by two-layer networks with good approximation properties. We refer to [46, Theorem 8] and [45, Theorem 4] for complete proofs.

**Proposition 3** (Approximation theorem). [46] Let  $f \in \mathcal{B}_1$ , and denote  $\rho = \rho(\epsilon)$  as its representing probability which satisfies  $c_\rho(f) \leq (1 + \epsilon) \|f\|_{\mathcal{B}_1}$  for some small  $\epsilon > 0$ , where

$$c_\rho(f) = \|f\|_{\mathcal{B}_{1,\rho}}. \quad (10)$$

Then, for any sample size  $n \in \mathbb{N}$ , there exists a probability  $\rho_n$ , a two-layer network  $f_n \in X_{n,c_\rho(f)}$  with  $\|f_n\|_{\mathcal{B}_1} \leq c_{\rho_n}(f_n) \leq c_\rho(f)$ , and a constant  $C(\Omega, d)$  depending only on the domain  $\Omega$  and dimensionality  $d$  such that

$$\|f - f_n\|_{H^1(\Omega)} \leq \frac{C(\Omega, d)}{\sqrt{n}} \|f\|_{\mathcal{B}_1}.$$

### III. EXPANDING NEURAL NETWORK METHODS

In this section, based on the method of expanding compacts [42], [43], we propose a new iterative regularization method, named as the *expanding neural network methods*. The proposed method is shown to converge to the unique exact solution  $f^\dagger$  to the equation  $A(f) = g$ , provided that  $A$  is a continuous injective operator. Our analysis considers two distinct scenarios based on the available *a priori* information about the quantity  $c_\rho(f^\dagger)$ , defined in (10).

A. *Case 1: given an energy bound of  $c_\rho(f^\dagger)$ .*

Let  $b : \mathbb{N}^+ \rightarrow \mathbb{N}^+$  be a monotonically increasing function such that there exists constants  $C_b, k_0 \geq 1$ :  $b(k+1) \leq C_b b(k)$  holds for all  $k \geq k_0$ . The first iterative regularization scheme is proposed in the following algorithm.

---

**Algorithm 1** An expanding neural network method for solving (1) with knowledge of  $c_\rho(f^\dagger)$

---

**Require:** Adaptive increasing sequence of neural networks  $b(k)$ , radius map  $r(n)$ , discrepancy parameter  $\tau > 1$ , noise level  $\delta$

**Ensure:** Reconstructed solution  $f_{n(\delta),k(\delta)}^\delta$ , suboptimal network size  $n(\delta)$ , iteration number  $k(\delta)$

1: **Initialization:**  $k \leftarrow 1, n \leftarrow b(1)$

2: Compute

$$f_{n,k}^\delta = \arg \min_{f \in X_{n,r(n)}} \|A(f) - g^\delta\|_{\mathcal{Y}}, \quad J_{n,k}^\delta = \|A(f_{n,k}^\delta) - g^\delta\|_{\mathcal{Y}} \quad (11)$$

3: **while**  $J_{n,k}^\delta > \tau\delta$  **do**

4:  $k \leftarrow k + 1$

5:  $n \leftarrow b(k)$

6: Update  $f_{n,k}^\delta$  and  $J_{n,k}^\delta$  by resolving (11) on the expanded class of neural networks  $X_{n,r(n)}$

7: **end while**

8: Set  $k(\delta) \leftarrow k, n(\delta) \leftarrow n$

9: **return**  $f_{n(\delta),k(\delta)}^\delta, n(\delta), k(\delta)$

---

The update rule  $n \leftarrow b(k)$  in the above algorithm provides a flexible strategy for increasing the network complexity. Typical choices include  $b(k) = k + 1$  (linear growth) or  $b(k) = k + m$  for some fixed constant  $m$  (fixed-step growth). The approximate solution  $f_{n,k}^\delta$  is obtained by solving a minimization problem constrained to a bounded compact set  $X_{n,r(n)}$ , which guarantees the existence of a regularized solution. As the algorithm progresses, the domain of the set  $X_{n,r(n)}$  expands with increasing  $n$ . This facilitates to search for more wider two layer networks until the algorithm is terminated by the well-known Morozov's discrepancy principle.

Now, we establish the convergence properties of Algorithm 1 in Theorem 1, the proof is provided in Appendix A. Under the assumption of prior information about the upper bound of  $c_\rho(f^\dagger)$  for the exact solution is known *a priori*, and provided that  $r(n)$  satisfies certain conditions, we show that the sequence generated by Algorithm 1 terminates after a finite number of steps and converges to the exact solution. Moreover, asymptotic estimates for both the stopping iteration and the number of neurons can be derived, which are directly linked to the degree of Hölder continuity of the forward operator  $A$ , as specified below.

**Definition 2.** We say that the operator  $A$  is locally Hölder continuous at  $f^\dagger$  of order  $\theta \in (0, 1]$  (with respect to the  $H^1$ -norm) if there exist constants  $L_A > 0$  and  $\gamma > 0$  such that

$$\|A(f) - A(f^\dagger)\|_{\mathcal{Y}} \leq L_A \|f - f^\dagger\|_{H^1(\Omega)}^\theta, \quad \text{for all } f \text{ with } \|f - f^\dagger\|_{H^1(\Omega)} < \gamma.$$

When  $\theta = 1$  this reduces to local Lipschitz continuity.

**Theorem 1.** Let  $A$  be a continuous injective operator, and  $r(n)$  be an increasing function that satisfies  $\lim_{n \rightarrow \infty} r(n) = B$ , where  $B$  is a fixed number such that  $B > c_\rho(f^\dagger)$ . Then,

- (Well-posedness of Algorithm 1) For any  $\delta > 0$  the iteration process in Algorithm 1 can be stopped at finite step  $k(\delta)$  with finite neurons  $n(\delta)$ , i.e.  $k(\delta) < +\infty, n(\delta) < +\infty$ . Moreover, if the operator  $A$  is locally Hölder continuous at  $f^\dagger$  of order  $\theta$ , then there exists a constant  $C > 0$ , independent of  $\delta$ , such that

$$k(\delta) \leq b^{-1}(C \delta^{-2/\theta}), \quad n(\delta) = \mathcal{O}(\delta^{-2/\theta})^1, \quad \text{as } \delta \rightarrow 0.$$

Here,  $b^{-1}$  denotes the (generalized) inverse of the monotonically increasing function  $b$ .

- (Regularization property of Algorithm 1) The approximate solutions  $f_{n(\delta),k(\delta)}^\delta$  converge to  $f^\dagger$  in  $H^1(\Omega)$  as  $\delta \rightarrow 0$ .

**Remark 1.** For typical choices of  $b = b(k)$  we obtain explicit rates. For instance, if  $b(k) \asymp k^{p^2}$  for some  $p > 0$ , then  $k(\delta) = \mathcal{O}(\delta^{-2/(p\theta)})$ ; if  $b(k) \asymp e^{qk}$  for some  $q > 0$ , then  $k(\delta) = \mathcal{O}(\log(1/\delta))$ .

<sup>1</sup>Throughout the paper we write  $f(\delta) = \mathcal{O}(g(\delta))$  as  $\delta \rightarrow 0$  if there exists a constant  $C > 0$ , independent of  $\delta$ , such that  $|f(\delta)| \leq C g(\delta)$  for all sufficiently small  $\delta > 0$ .

<sup>2</sup>We write  $f \asymp g$  if there exist constants  $0 < c \leq C < \infty$ , independent of the argument, such that  $cg(x) \leq f(x) \leq Cg(x)$  for all  $x$  in the domain under consideration..

*B. Case 2: without knowledge of  $c_\rho(f^\dagger)$*

Now, we consider the inverse problem without any prior knowledge of the quantity  $c_\rho(f^\dagger)$ . To compensate for this, our analysis requires the forward operator  $A$  to satisfy the  $\theta$ -degree Hölder continuity as given in Definition 2, and the introduction of a penalty term  $\mathcal{R}$  in the corresponding optimization problem. This additional term  $\mathcal{R}$  ensures the uniform boundedness of the minimizer throughout the iterations. To this end, we present the following algorithm, which closely resembles Algorithm 1.

---

**Algorithm 2** The modified expanding neural network method for solving equation (1)

---

**Require:** Adaptive increasing sequence of neural networks  $b(k)$ , radius map  $r(n)$ , discrepancy parameter  $\tau > 1$ , regularization parameters  $c_0 > 0$ ,  $\theta > 0$ , regularization penalty  $\mathcal{R}$ , noise level  $\delta$

**Ensure:** Reconstructed solution  $f_{n(\delta),k(\delta)}^\delta$ , suboptimal network size  $n(\delta)$ , iteration number  $k(\delta)$

1: **Initialization:**  $k \leftarrow 1$ ,  $n \leftarrow b(1)$

2: Set  $\beta_n = c_0 n^{-\theta/2}$  and compute

$$f_{n,k}^\delta = \arg \min_{f \in X_{n,r(n)}} \left( \|A(f) - g^\delta\|_{\mathcal{Y}} + \beta_n \mathcal{R}(f) \right), \quad J_{n,k}^\delta = \|A(f_{n,k}^\delta) - g^\delta\|_{\mathcal{Y}}. \quad (12)$$

3: **while**  $J_{n,k}^\delta > \tau \delta$  **do**

4:    $k \leftarrow k + 1$

5:    $n \leftarrow b(k)$

6:   Update  $\beta_n = c_0 n^{-\theta/2}$

7:   Update  $f_{n,k}^\delta$  and  $J_{n,k}^\delta$  by resolving (12) on the expanded class of neural networks  $X_{n,r(n)}$

8: **end while**

9: Set  $n(\delta) \leftarrow n$ ,  $k(\delta) \leftarrow k$

10: **return**  $f_{n(\delta),k(\delta)}^\delta$ ,  $n(\delta)$ ,  $k(\delta)$

---

The corresponding convergence properties of Algorithm 2, including its well-posedness and regularization behavior, are established in Theorem 2. The result demonstrates that this modified algorithm can produce a sequence of regularized solutions converging to the exact solution in the appropriate function space, without requiring additional conditions on  $r(n)$ . The proof of Theorem 2 is provided in Appendix B.

**Theorem 2.** *Let  $A$  be a continuous injective operator that is locally Hölder continuous at  $f^\dagger$  of order  $\theta \in (0, 1]$  (as in Definition 2) with constants  $L_A > 0$  and  $\gamma_1 > 0$ . Assume one of the following holds for the regularizer  $\mathcal{R}$ :*

(i)  $\mathcal{R} = \mathcal{R}_1$  is locally Hölder continuous at  $f^\dagger$  of the same order  $\theta$ , with constants  $L_{\mathcal{R}_1} > 0$  and  $\gamma_2 > 0$ , and there exists  $C_{\mathcal{R}_1} > 0$  such that  $C_{\mathcal{R}_1} \|f\|_{H^1(\Omega)} \leq \mathcal{R}_1(f) < +\infty$ .

(ii)  $\mathcal{R} = \mathcal{R}_2$  with  $\mathcal{R}_2(f_n) = c_{\rho_n}(f_n)$  for  $f_n \in X_{n,r(n)}$ ,  $r(n) > 0$ .

Then, the following hold

- (Well-posedness of Algorithm 2) For any  $\delta > 0$  the iteration process in Algorithm 2 can be stopped at finite step  $k(\delta)$  with finite neurons  $n(\delta)$ , i.e.  $k(\delta) < +\infty$ ,  $n(\delta) < +\infty$ . Moreover, there exists a constant  $C > 0$ , independent of  $\delta$ , such that

$$k(\delta) \leq b^{-1}(C \delta^{-2/\theta}), \quad n(\delta) = \mathcal{O}(\delta^{-2/\theta}), \quad \text{as } \delta \rightarrow 0.$$

- (Regularization property of Algorithm 2) The approximate solutions  $f_{n(\delta),k(\delta)}^\delta$  converge to  $f^\dagger$  as  $\delta \rightarrow 0$ , namely,

$$f_{n(\delta),k(\delta)}^\delta \rightarrow f^\dagger \quad \text{in } L^2(\Omega) \text{ if } \mathcal{R} = \mathcal{R}_1, \quad f_{n(\delta),k(\delta)}^\delta \rightarrow f^\dagger \quad \text{in } H^1(\Omega) \text{ if } \mathcal{R} = \mathcal{R}_2.$$

Theorems 1 and 2 indicate that the proposed algorithms provide a constructive strategy for building neural networks that serve as regularization solutions, offering explicit answers to the foundational questions (Q1-Q3) from the introduction:

- **Answer to Q1:** the algorithm is designed to construct a neural network that yields a stable approximation for ill-posed problems. The stopping criterion, based on the discrepancy principle, ensures the solution's regularity in the presence of noisy data. The number of neurons  $n$  functions both as the regularization parameter as well as the iteration steps.
- **Answer to Q2:** our theorems derive a quantitative relationship between the sufficient network size  $n = n(\delta)$  and the noise level  $\delta$ . Specifically, under the condition that the operator  $A$  is locally Hölder continuous of order  $\theta$ , this relationship is quantitatively described by  $n(\delta) = \mathcal{O}(\delta^{-2/\theta})$ . This result theoretically confirms that a larger network is not always beneficial. Moreover, the numerical results in Section V will empirically validate that for higher noise levels, the approximation error does not decrease monotonically as the number of neurons increases.
- **Answer to Q3:** the expanding neural network methodology progressively increases the number of neurons  $n$ , thereby inherently incorporating a mechanism for identifying a two-layer neural network of minimal sufficient width that meets the stopping criterion. The algorithm automatically selects a suitable network size  $n$  to achieve a compromise between computational complexity and approximation accuracy.

#### IV. A NEURAL NETWORK-BASED TIKHONOV REGULARIZATION SCHEME

This section addresses a method different from the expanding neural network scheme discussed earlier. In the previous framework, the number of neurons  $n$  serves as an implicit regularization parameter, making the quality of the solution highly sensitive to the choice of stopping criterion. By contrast, the variational regularization framework developed here incorporates an explicit parameter  $\alpha$ , providing more direct and stable control over the solution. While inspired by the general principles of variational regularization [40], our theory is established independently within the neural network setting. We propose a neural network-based Tikhonov regularization scheme to address the ill-posed problem (1). Within this framework, we establish convergence of the regularized solutions and, under standard variational source conditions, derive explicit convergence rates that characterize the efficiency of the method. The core idea of our scheme is to seek two layer neural networks as the regularized solution that are obtained as the minimizer of the functional

$$f_{n,\alpha}^\delta := \arg \min_{f \in X_{n,\infty}} \mathcal{T}_\alpha(f, g^\delta), \quad \mathcal{T}_\alpha(f, g^\delta) = \mathcal{D}(A(f), g^\delta) + \alpha \mathcal{P}(f), \quad (13)$$

where  $X_{n,\infty}$  is defined in (9),  $\mathcal{D} : (\mathcal{Y}, \mathcal{Y}) \rightarrow \mathbb{R}_+$  is an appropriate similarity measure in the data space enforcing data consistency,  $\alpha > 0$  is the regularization parameter and  $\mathcal{P}(f) : X_{n,\infty} \rightarrow \mathbb{R}_+$  is the regularization stabilizer term, which is designed here by

$$\mathcal{P}(f) := \varphi(c_{\rho_n}(f)), \quad c_{\rho_n}(f) \equiv \frac{1}{n} \sum_{i=1}^n |a_i| (\|\mathbf{b}_i\|_1 + |c_i|), \quad (14)$$

where  $\varphi : X_{n,\infty} \rightarrow \mathbb{R}_+$  is a non-negative functional. To this end, we summarize the main assumptions underlying Tikhonov regularization (13). These assumptions are standard within the regularization theory of abstract inverse problems formulated in normed spaces; see, for instance, [47].

**Assumption 1.**(A1) *Data consistency term  $\mathcal{D} : (\mathcal{Y}, \mathcal{Y}) \rightarrow \mathbb{R}_+$  and forward operator  $A$  satisfy the following five conditions:*

- 1) *For some  $\tau \geq 1$  we have  $\forall g_0, g_1, g_2 \in \mathcal{Y} : \mathcal{D}(g_0, g_1) \leq \tau \mathcal{D}(g_0, g_2) + \tau \mathcal{D}(g_2, g_1)$ ;*
- 2)  *$\forall g_0, g_1 \in \mathcal{Y} : \mathcal{D}(g_0, g_1) = 0 \iff g_0 = g_1$ ;*
- 3)  *$\forall \{g_k\}_{k=1}^\infty \subset \mathcal{Y} : g_k \rightarrow g \implies \mathcal{D}(g_k, g) \rightarrow 0$ ;*
- 4) *The functional  $(f, g) \mapsto \mathcal{D}(A(f), g)$  is sequentially lower semi-continuous with respect to  $f$  and  $g$ ;*
- 5) *For any  $f' \in \mathcal{B}_1$  and exact solution  $f^* \in \mathcal{B}_1$  of  $A(f) = g$ , it holds that*

$$\mathcal{D}(A(f'), g) \leq K_A \|f' - f^*\|_{H^1(\Omega)}^s \quad (15)$$

*for some constants  $s, K_A \geq 0$ .*

(A2)  $\varphi : X_{n,\infty} \rightarrow \mathbb{R}_+$  *is a continuous increasing function.*

Note that the squared norm  $\|\cdot\|_{L^2(\Omega)}^2$  satisfies Condition (A1) when  $A$  is an  $L_A$ -Lipschitz continuous operator. Specifically, conditions (A1.1)-(A1.3) in Assumption 1 are straightforward to verify, while (A1.4) and (A1.5) hold with  $K_A = L_A^2$  and  $s = 2$ , as guaranteed by the Lipschitz continuity of  $A$  and Proposition 2.

We are now in a position to demonstrate that the Tikhonov regularization method is a well-posed and convergent scheme, characterized by existence, stability, and convergence. In particular, Theorem 3 establishes that, by employing (13), one can construct a sequence that converges to a  $\mathcal{R}$ -minimizing solution defined in (17), as  $n \rightarrow \infty$  and  $\delta \rightarrow 0$ , provided that the regularization parameter is chosen appropriately as in (16). The proof of Theorem 3 is provided in Appendix C.

**Theorem 3** (Well-posedness). *Let Assumption 1 be satisfied. The following assertions hold true:*

- (a) *Existence: for each  $n \in \mathbb{N}$ , every  $g \in \mathcal{Y}$  and every  $\alpha > 0$ , there exists a minimizer  $f_n^*$  of  $\mathcal{T}_\alpha(f, g)$  in  $X_{n,\infty}$ .*
- (b) *Stability: let  $n \in \mathbb{N}$  and  $\alpha > 0$  be fixed. If  $g_k \rightarrow g$  as  $k \rightarrow \infty$  and  $f_{n,k} \in \arg \min_{f \in X_{n,\infty}} \mathcal{T}_\alpha(f, g_k)$ , then there exist a subsequence  $\{f_{n,k_\ell}\}_{\ell=1}^\infty$  and some  $f_n^* \in \arg \min_{f \in X_{n,\infty}} \mathcal{T}_\alpha(f, g)$  such that*

$$f_{n,k_\ell} \rightarrow f_n^* \quad \text{in } L^2(\Omega), \quad \text{as } \ell \rightarrow \infty.$$

- (c) *Convergence: let  $f \in \mathcal{B}_1$  and  $g := A(f)$ . Let  $\{g_k\}_{k=1}^\infty \subset \mathcal{Y}$  satisfy  $\mathcal{D}(g, g_k) \leq \delta_k$  for some sequence  $\delta_k \searrow 0$  as  $k \rightarrow \infty$ . For each  $n, k \in \mathbb{N}$ , let  $\alpha_{k,n} > 0$  be a regularization parameter and choose  $f_{n,k} \in \arg \min_{f \in X_{n,\infty}} \mathcal{T}_{\alpha_{k,n}}(f, g_k)$ . Assume that the parameter choice  $\alpha_{k,n} = \alpha(\delta_k, n)$  satisfies*

$$\alpha_{k,n} \rightarrow 0, \quad \alpha_{k,n}^{-1}(\delta_k + n^{-s/2}) \rightarrow 0 \quad \text{as } \delta_k \rightarrow 0, \quad n \rightarrow \infty. \quad (16)$$

*Then there exists a subsequence  $\{f_{n,k_\ell}\}_{n,\ell}$  such that*

$$f_{n,k_\ell} \rightarrow f^\dagger \quad \text{in } L^2(\Omega), \quad \text{as } n, \ell \rightarrow \infty,$$

*where  $f^\dagger$  is an  $\mathcal{R}$ -minimizing solution of (1), i.e.*

$$f^\dagger \in \arg \min \{ \mathcal{R}(f) := \varphi(\|f\|_{\mathcal{B}_1}) \mid f \in \mathcal{B}_1, A(f) = g \}. \quad (17)$$

We next derive convergence rates results about the Tikhonov regularization method. It is well-known that under general assumptions (specifically, Assumption 1), the convergence rate of  $f_n \rightarrow f^\dagger$  as  $n \rightarrow \infty$  for precise data, and of  $f_{n,k_\ell} \rightarrow f^\dagger$  as  $n, \ell \rightarrow \infty$  for noisy data, can be arbitrarily slow if the exact solution  $f^\dagger$  lacks sufficient smoothness (cf. [23]). Consequently, establishing convergence rates typically requires imposing appropriate smoothness conditions on the exact solution. Commonly used smoothness conditions include range-type source conditions (see, e.g., [48]–[50]), approximate source conditions (see [51]), and variational source conditions, which take the form of variational inequalities (see [52]). In what follows, we focus specifically on variational source conditions, as these represent the weakest assumptions under which convergence rate results can still be derived.

**Assumption 2** (Variational source condition). *Let  $f^* \in \mathcal{B}_1$  be a solution of  $A(f) = g$ . There exist a radius  $\epsilon > 0$ , an error measure functional  $\mathcal{E}^\dagger : \mathcal{B}_1 \rightarrow [0, \infty]$  with  $\mathcal{E}^\dagger(f^*) = 0$  and a concave index function<sup>3</sup>  $\Phi : [0, \infty) \rightarrow [0, \infty)$  such that for all  $f \in \mathcal{B}_1$  with  $\|f - f^*\|_{L^2(\Omega)} < \epsilon$ ,*

$$\mathcal{E}^\dagger(f) \leq \mathcal{R}(f) - \mathcal{R}(f^*) + \Phi(D(A(f), g)).$$

By Assumption 2, we are able to obtain the convergence rates results, as shown in Theorem 4, the proof of which is given in Appendix D.

**Theorem 4** (Convergence rates). *Let Assumption 1 hold, and let  $f^\dagger$  in (17) satisfy Assumption 2. Moreover, let  $g^\delta \in \mathcal{Y}$  satisfy  $\mathcal{D}(g, g^\delta) \leq \delta$  for some  $\delta > 0$ . Then, for any minimizer*

$$f_{n,\alpha}^\delta(\mathbf{x}) = \frac{1}{n} \sum_{i=1}^n a_{i,\alpha}^\delta \left( \mathbf{b}_{i,\alpha}^\delta \cdot \mathbf{x} + c_{i,\alpha}^\delta \right)_+ = \arg \min_{f \in X_{n,\infty}} \mathcal{T}_\alpha(f, g^\delta) \quad (18)$$

contains a subsequence, still denoted by  $\{f_{n,\alpha}^\delta\}$  for simplicity, such that  $f_{n,\alpha}^\delta \rightarrow f^\dagger$  in  $L^2(\Omega)$  as  $n \rightarrow \infty$  and  $\delta \rightarrow 0$ . In addition, the following statements hold.

(i) for any sufficient small  $\alpha, \delta$ , we have

$$\mathcal{E}^\dagger(f_{n,\alpha}^\delta) \leq \tau \alpha^{-1} (\delta + C n^{-\frac{5}{2}}) + \Phi(\tau \delta) + \tau^{-1} \Phi^*(\tau \alpha), \quad (19)$$

$$\|f_{n,\alpha}^\delta\|_{\mathcal{B}_1} \leq \varphi^{-1} (\tau \alpha^{-1} (\delta + C n^{-\frac{5}{2}}) + \varphi(\|f^\dagger\|_{\mathcal{B}_1})), \quad (20)$$

where  $C = K_A(C(\Omega, d)\|f\|_{\mathcal{B}_1})^s$ , and  $\Phi^*$  denotes the (generalized) inverse of the Fenchel conjugate  $\Phi^*$  of  $\Phi$ , defined by  $\Phi^*(\alpha) := \sup_{t \geq 0} \{\alpha t - \Phi(t)\}$ .

(ii) if  $n(\delta) \asymp \delta^{-2/s}$ ,  $\alpha(\delta) \asymp \delta/\Phi(\tau\delta)$ , we have  $\mathcal{E}^\dagger(f_{n(\delta),\alpha(\delta)}^\delta) = \mathcal{O}(\Phi(\tau\delta))$ .

In particular, when  $\Phi(t) = c_0 t^\mu$  with  $0 < \mu < 1$ , the choices  $n(\delta) \asymp \delta^{-2/s}$ ,  $\alpha(\delta) \asymp \delta^{1-\mu}$  yields the rate  $\mathcal{E}^\dagger(f_{n(\delta),\alpha(\delta)}^\delta) = \mathcal{O}(\delta^\mu)$ .

Theorem 4 yields quantitative convergence rates for the regularized solutions  $f_{n,\alpha}^\delta$ : under a variational source condition, the error measured by the functional  $\mathcal{E}^\dagger$  can be controlled in terms of  $\alpha, \delta$  and the index function  $\Phi$ , and, for  $\Phi(t) = c_0 t^\mu$  with  $0 < \mu < 1$ , one obtains the rate  $\mathcal{E}^\dagger(f_{n,\alpha}^\delta) = \mathcal{O}(\delta^\mu)$  together with the  $\mathcal{B}_1$ -norm bound (20).

For the specific data consistency term  $\mathcal{D}(A(f), g) = \|A(f) - g\|_{L^2(\Omega)}^2$ , we present the following corollary. It summarizes the corresponding convergence properties established in Theorem 3 and the convergence rates derived in Theorem 4.

**Corollary 1.** *Suppose that the forward operator  $A$  of (1) is  $L_A$ -Lipschitz continuous, and that  $f^\dagger$  in (17) satisfies a certain variational source condition 2 with  $\mathcal{E}^\dagger(f) = \|f - f^\dagger\|_{L^2(\Omega)}^2$ , i.e., there exists an index function  $\Phi$  such that for all  $f \in \mathcal{B}_1$  with  $\|f - f^\dagger\|_{L^2(\Omega)} < \epsilon$  (for some  $\epsilon > 0$ ) it holds*

$$\|f - f^\dagger\|_{L^2(\Omega)}^2 \leq \|f\|_{\mathcal{B}_1}^2 - \|f^\dagger\|_{\mathcal{B}_1}^2 + \Phi(\|A(f) - A(f^\dagger)\|_{L^2(\Omega)}^2).$$

Let  $g^\delta \in \mathcal{Y}$  satisfy  $\|g - g^\delta\|_{\mathcal{Y}}^2 \leq \delta$  for some  $\delta > 0$ . For  $n \in \mathbb{N}$  and  $\alpha > 0$ , let

$$f_{n,\alpha}^\delta(\mathbf{x}) = \frac{1}{n} \sum_{i=1}^n a_{i,\alpha}^\delta \left( \mathbf{b}_{i,\alpha}^\delta \cdot \mathbf{x} + c_{i,\alpha}^\delta \right)_+ = \arg \min_{f \in X_{n,\infty}} \mathcal{T}_\alpha(f, g^\delta). \quad (21)$$

Then the following hold:

- (Convergence) If the parameter choice  $\alpha = \alpha(\delta, n)$  satisfy

$$\alpha \rightarrow 0, \quad \alpha^{-1}(\delta + n^{-1}) \rightarrow 0, \quad \text{as } n \rightarrow \infty, \quad \delta \rightarrow 0,$$

then there exists a convergent subsequence (still denoted by  $\{f_{n,\alpha}^\delta\}$ ) which converges in  $L^2(\Omega)$  to an  $\mathcal{R}$ -minimizing solution of  $A(f) = g$ .

<sup>3</sup> $\Phi$  is called an index function if it is continuous and strictly increasing with  $\Phi(0) = 0$ .

- (Convergence rate) If the parameters are chosen such that  $n(\delta) \asymp \delta^{-1}$  and  $\alpha(\delta) \asymp \delta/\Phi(\tau\delta)$ , then it follows that  $\|f_{n(\delta),\alpha(\delta)}^\delta - f^\dagger\|_{L^2(\Omega)} = \mathcal{O}(\sqrt{\Phi(\tau\delta)})$ . In particular, if  $\Phi(t) = c_0 t^\mu$  with  $c_0 > 0$  and  $0 < \mu < 1$ , then the choices  $n(\delta) \asymp \delta^{-1}$  and  $\alpha(\delta) \asymp \delta^{1-\mu}$  yields the rate  $\|f_{n(\delta),\alpha(\delta)}^\delta - f^\dagger\|_{L^2(\Omega)} = \mathcal{O}(\delta^{\mu/2})$ .

*Proof.* These conclusions follow naturally from a combination of Theorem 3 and Theorem 4 by letting the data consistency term  $\mathcal{D}(A(f), g) = \|A(f) - g\|_{L^2(\Omega)}^2$  with  $s = 2, K_A = L_A^2$ .  $\square$

The convergence rate results established in Theorem 4, along with Corollary 1, imply an optimal choice for the number of neurons, thereby providing explicit answers to the foundational question **(Q4)** posed in the introduction.

- **Answer to Q4:** Under a general variational source condition, our network-based Tikhonov scheme admits the convergence rate  $\Phi(\tau\delta)$ , which coincides with the rates known for classical regularization under variational source conditions [53]. Moreover, we quantify the network size required to realize this rate together with an appropriate choice of the regularization parameter, namely  $n(\delta) \asymp \delta^{-2/s}$ , as established in Theorem 4.

## V. NUMERICAL EXPERIMENTS

In this section, we present three numerical examples to verify the theoretical results discussed in the previous sections. The numerical experiments follow the procedure outlined below, and all relevant data and source code are publicly available on GitHub at <https://github.com/z1998w/DNNip>.

The numerical experiments briefly consist of the following four steps:

- 1) As a reference solution we generate the exact function  $f^\dagger$  of the form (cf. [46])

$$f^\dagger(t) = \sum_{j=1}^T \phi_j K_d(t, \ell^j), \quad t \in [0, 1]^d, \quad (22)$$

where  $K_d$  is the polynomial kernel defined by  $K_d(t, \ell) = \langle t, \ell \rangle_{\mathbb{R}^d} + 1$ , for  $t \in [0, 1]^d$ . Unless otherwise specified, the nodes  $\ell^j = (\ell_1^j, \ell_2^j, \dots, \ell_d^j)$  and coefficients  $\phi_j$  (for  $j = 1, \dots, T$ ) were independently and uniformly drawn from the cubes  $[-1, 1]^d$  and  $[-1, 1]$  respectively. For each example below, appropriate modifications were made to this construction to suit specific purposes.

- 2) Compute the exact data  $g = A(f^\dagger)$ , and generate the noise data  $g^\delta$  by

$$g^\delta = g + \delta \cdot \xi,$$

where  $\delta$  is the noise level and  $\xi$  is uniformly distributed in  $[-1, 1]$ .

- 3) Approximate the exact solution  $f^\dagger$  by two-layer networks

$$f = \frac{1}{n} \sum_{j=1}^n a_j \left( \mathbf{b}_j^T \mathbf{x} + c_j \right)_+ \in X_{n,r(n)},$$

which consists of solving the following three minimization problems:

- Algorithm 1: let  $r(n)$  be an increasing sequence bounded a constant  $B \geq c_{\rho_n}(f^\dagger) = \|\sum_{j=1}^T \phi_j \ell^j\|_1 + |\sum_{j=1}^T \phi_j|$ ,

$$\min_{\substack{(a_j, \mathbf{b}_j, c_j) \in M_{r(n)}, \\ j=1, \dots, n}} \left\| A \left( \frac{1}{n} \sum_{j=1}^n a_j \left( \mathbf{b}_j^T \mathbf{x} + c_j \right)_+ \right) - g^\delta \right\|_{\mathcal{Y}},$$

where  $M_r := \{(a_j, \mathbf{b}_j, c_j) \in \mathbb{R} \times \mathbb{R}^d \times \mathbb{R}, |a_j| \leq r(n), \|\mathbf{b}_j\|_1 + |c_j| = 1\}$ .

- Algorithm 2: take  $\mathcal{R}(f) = \mathcal{R}_1(f) = C_{\mathcal{R}_1} \|f\|_{H^1(\Omega)}$  that is a  $C_{\mathcal{R}_1}$ -Lipschitz continuous majorant functional of the  $H^1$  norm,

$$\min_{\substack{(a_j, \mathbf{b}_j, c_j) \in M_{r(n)}, \\ j=1, \dots, n}} \left\| A \left( \frac{1}{n} \sum_{j=1}^n a_j \left( \mathbf{b}_j^T \mathbf{x} + c_j \right)_+ \right) - g^\delta \right\|_{\mathcal{Y}} + \beta_n a \left\| \frac{1}{n} \sum_{j=1}^n a_j \left( \mathbf{b}_j^T \mathbf{x} + c_j \right)_+ \right\|_{H^1(\Omega)},$$

where  $\beta_n = c_0 n^{-\frac{\theta}{2}}$ , and  $c_0 = C_{\mathcal{R}_1} = 0.1, \theta = 1$ .

- Tikhonov regularization:

$$\min_{\substack{(a_j, \mathbf{b}_j, c_j) \in M_\infty, \\ j=1, \dots, n}} \left\| A \left( \frac{1}{n} \sum_{j=1}^n a_j \left( \mathbf{b}_j^T \mathbf{x} + c_j \right)_+ \right) - g^\delta \right\|_{\mathcal{Y}}^2 + \alpha \left( \frac{1}{n} \sum_{j=1}^n |a_j| (\|\mathbf{b}_j\|_1 + |c_j|) \right)^2,$$

here the regularization parameter  $\alpha$  is a small positive number chosen by

$$\alpha = (\delta + n^{-1})^\eta, \quad \eta = 0.8.$$

- 4) To quantify the accuracy of the regularized solutions  $f_n^\delta$ , we consider the relative  $L^2$ -error with respect to the exact solution  $f^\dagger$ , defined by

$$\text{Relative } L^2 \text{ Error} := \frac{\|f_n^\delta - f^\dagger\|_{L^2([0,1]^d)}}{\|f^\dagger\|_{L^2([0,1]^d)}} \approx \frac{\sqrt{\sum_{i=1}^N (f_n^\delta(t_i) - f^\dagger(t_i))^2}}{\sqrt{\sum_{i=1}^N (f^\dagger(t_i))^2}}. \quad (23)$$

We now detail the numerical implementation common to all experiments. All continuous problems are discretized: the solution  $f$  is represented on an  $N$ -point solution grid and the noisy data  $g^\delta$  on an  $M$ -point data grid. The continuous norms in the objective functionals are approximated by standard numerical quadrature on these grids. The resulting non-convex optimization problems are solved with the Adam optimizer with a fixed learning rate of  $10^{-3}$ . To balance expressive capacity and training efficiency, we adopt a progressive width schedule: the number of neurons  $n$  starts at 50 and is increased in steps of 20 up to a prescribed maximum  $n_{\max}$ . This expansion is accelerated by a warm-start strategy, where the parameters of existing neurons are retained and only the parameters of newly added neurons are randomly initialized. The specific discretization parameters and training iterations are chosen as follows. For Examples 1-2 (1D problems) we set  $N = 101$  ( $M = 51$  for Example 1,  $M = 101$  for Example 2),  $n_{\max} = 1000$ , and train for 600 (Algorithms 1, 2) or 1200 (Tikhonov) iterations per increment of  $n$ . For Example 3 (2D problem) we set  $N = 31^2 = 961$ ,  $M = 124$ ,  $n_{\max} = 500$ , and train for 1500 (Algorithms 1, 2) or 2500 (Tikhonov) iterations per increment. The robustness of the observed trends is assessed by repeating all experiments for several random seeds. In the figures below, the horizontal axis (number of neurons  $n$ ) is plotted on a base-10 logarithmic scale in order to emphasize the initial steep reduction of the error.

**Remark 2.** Note that the exact solution  $f^\dagger$  generated by (22) lies in the Barron space  $\mathcal{B}_1$ , since it admits the representation (7) with respect to the uniform probability measure  $\rho_n$  with  $n = d + 1$ . Writing

$$f^\dagger(t) = u^T t + v, \quad u := \sum_{j=1}^T \phi_j \ell^j \in \mathbb{R}^d, \quad v := \sum_{j=1}^T \phi_j,$$

and choosing  $\rho_n$  uniform on the  $d + 1$  atoms

$$(a_k, \mathbf{b}_k, c_k) = (nu_k, e_k, 0) \quad (k = 1, \dots, d), \quad (a_0, \mathbf{b}_0, c_0) = (nv, \mathbf{0}, 1),$$

we obtain an explicit Barron representation with respect to  $\rho_n$ , and the corresponding Barron norm is

$$c_{\rho_n}(f^\dagger) = \|f^\dagger\|_{\mathcal{B}_1, \rho_n} = \mathbb{E}_{\rho_n} [|a|^p (\|\mathbf{b}\|_1 + |c|)^p] = \sum_{k=1}^d |u_k| + |v| = \left\| \sum_{j=1}^T \phi_j \ell^j \right\|_1 + \left| \sum_{j=1}^T \phi_j \right|.$$

**Example 1.** 1D Fredholm integral equation of the first kind:

$$A(f) = \int_0^1 K(t, s) f(s) ds = g(t), \quad t \in [0, 1], s \in [0, 1],$$

where

$$K(t, s) = \begin{cases} s(1-t), & 0 \leq s \leq t \leq 1, \\ t(1-s), & 0 \leq t < s \leq 1. \end{cases}$$

The operator  $A$  is linear, compact, and self-adjoint on  $L^2[0, 1]$ . Its eigenvalues are  $\lambda_n = 1/(n^2\pi^2)$  with corresponding eigenfunctions  $\sin(n\pi t)$ , which implies that  $A$  is injective. Moreover, as a bounded linear operator with  $\|A\| = 1/\pi^2$ , it is globally Lipschitz continuous. These properties ensure that the assumptions of Theorems 1 and 2 are satisfied. In this example, the exact solution  $f^\dagger$  is constructed by (22) with  $T = 10$  and  $d = 1$ .

**Example 2.** 1D auto-convolution Volterra integral equations (AVIEs) of the first kind:

$$A(f) = \int_0^t f(t-s) f(s) ds = g(t), \quad t \in [0, 1]. \quad (24)$$

Here,  $A$  is a nonlinear continuous operator. According to [54], [55], the auto-convolution operator is not injective (e.g.  $A(f) = A(-f)$ ). However, when restricted to the cone of strictly nonnegative functions (e.g.  $f \in C[0, 1]$  with  $f > 0$ ),  $A$  is injective. Furthermore, for any  $f, f^\dagger \in H^1(\Omega)$  with  $\|f - f^\dagger\|_{H^1(\Omega)} \leq \gamma$ , the following local Lipschitz estimate holds according to the Young's inequality:

$$\|A(f) - A(f^\dagger)\|_{L^2(0,1)} \leq (\|f\|_{L^1(0,1)} + \|f^\dagger\|_{L^1(0,1)}) \|f - f^\dagger\|_{L^2(0,1)}$$

By Sobolev embedding,  $\|u\|_{L^1(\Omega)} \leq C_\Omega \|u\|_{H^1(\Omega)}$  and  $\|u\|_{L^2(\Omega)} \leq C_\Omega \|u\|_{H^1(\Omega)}$  for some constant  $C_\Omega > 0$ . Together with the bound  $\|f\|_{H^1(\Omega)} \leq \|f^\dagger\|_{H^1(\Omega)} + \gamma$ , we obtain

$$\|A(f) - A(f^\dagger)\|_{L^2(0,1)} \leq C_\Omega^2 (2\|f^\dagger\|_{H^1(\Omega)} + \gamma) \|f - f^\dagger\|_{H^1(\Omega)}.$$

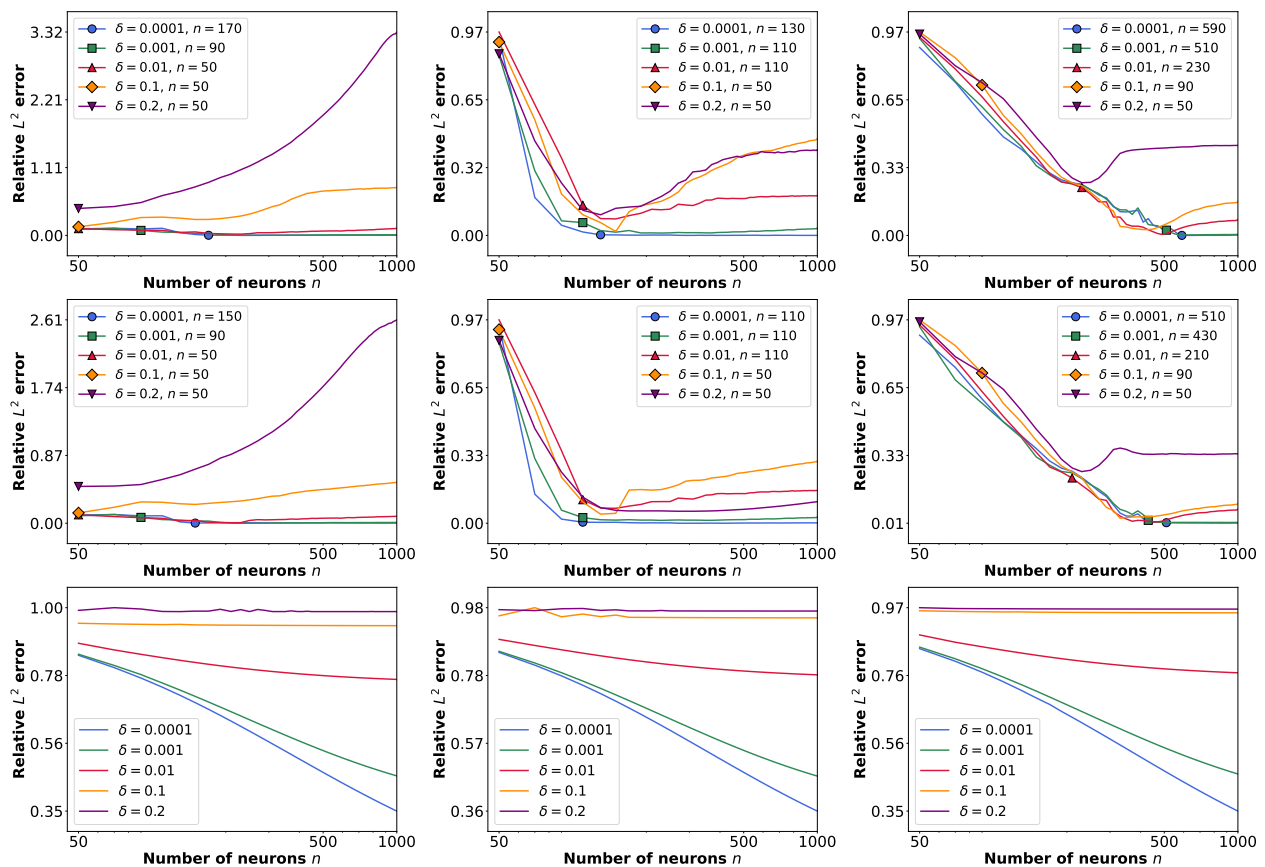


Fig. 1. 1D linear integral equation: Relative  $L^2$  error of  $f_n^\delta$  obtained by Algorithm 1 (top row), Algorithm 2 (middle row), and Tikhonov regularization (bottom row). Each column corresponds to a different random seed: 111, 666, 3333 (from left to right). The marker on each curve highlights the first network architecture that satisfied the stopping criterion for each noise level, with  $\tau = 1.0001$ . The corresponding value of  $n$  (the stopping number) is indicated in the legend.

Thus,  $A$  is locally Lipschitz at any  $f^\dagger \in H^1(\Omega)$ , and Example 2 meets the assumptions of Theorems 1-2. For this example, to ensure a nonnegative exact solution, we define the exact solution  $f^\dagger$  according to (22), where  $\ell^j, \phi_j$  were uniformly drawn from the cubes  $[0, 1]^d$  and  $[0, 1]$  respectively, and we set  $T = 5, d = 1$ .

**Example 3.** The 2D equation of electrical impedance tomography (EIT) [31] is considered on the unit square domain  $\Omega = [0, 1]^2$ :

$$\nabla \cdot (f(x, y) \nabla u(x, y)) = 0, \quad (x, y) \in \Omega, \quad (25)$$

where  $f(x, y)$  denotes the electrical conductivity, while  $u(x, y)$  means the electrical potential. A voltage distribution, denoted by  $h(x, y)$ , is applied on the boundary  $\partial\Omega$ , corresponding to the Dirichlet boundary condition  $u(x, y)|_{\partial\Omega} = h(x, y)$ . This applied voltage induces a boundary current flux  $g(x, y)$ , which is then measured as the Neumann boundary data:

$$g(x, y) = f(x, y) \frac{\partial u}{\partial \nu}(x, y), \quad (x, y) \in \partial\Omega,$$

where  $\nu$  is the unit outward normal vector to  $\partial\Omega$ . The Dirichlet-to-Neumann (DN) map is the operator that maps any applied voltage to the resulting measured current:

$$\Lambda_f : u(x, y)|_{\partial\Omega} \mapsto (f(x, y) \frac{\partial u}{\partial \nu}(x, y))|_{\partial\Omega}.$$

The forward problem in EIT is to compute the boundary current  $g$  corresponding to a given conductivity distribution  $f$  and a specified voltage  $h$ . The classical inverse problem in EIT, known as Calderón's problem, seeks to reconstruct  $f$  from the complete DN map  $\Lambda_f$ . It is well established that the DN map uniquely determines an isotropic, essentially bounded conductivity. Consequently, the forward operator  $A : f \mapsto \Lambda_f$  is injective at  $f^\dagger$  [56].

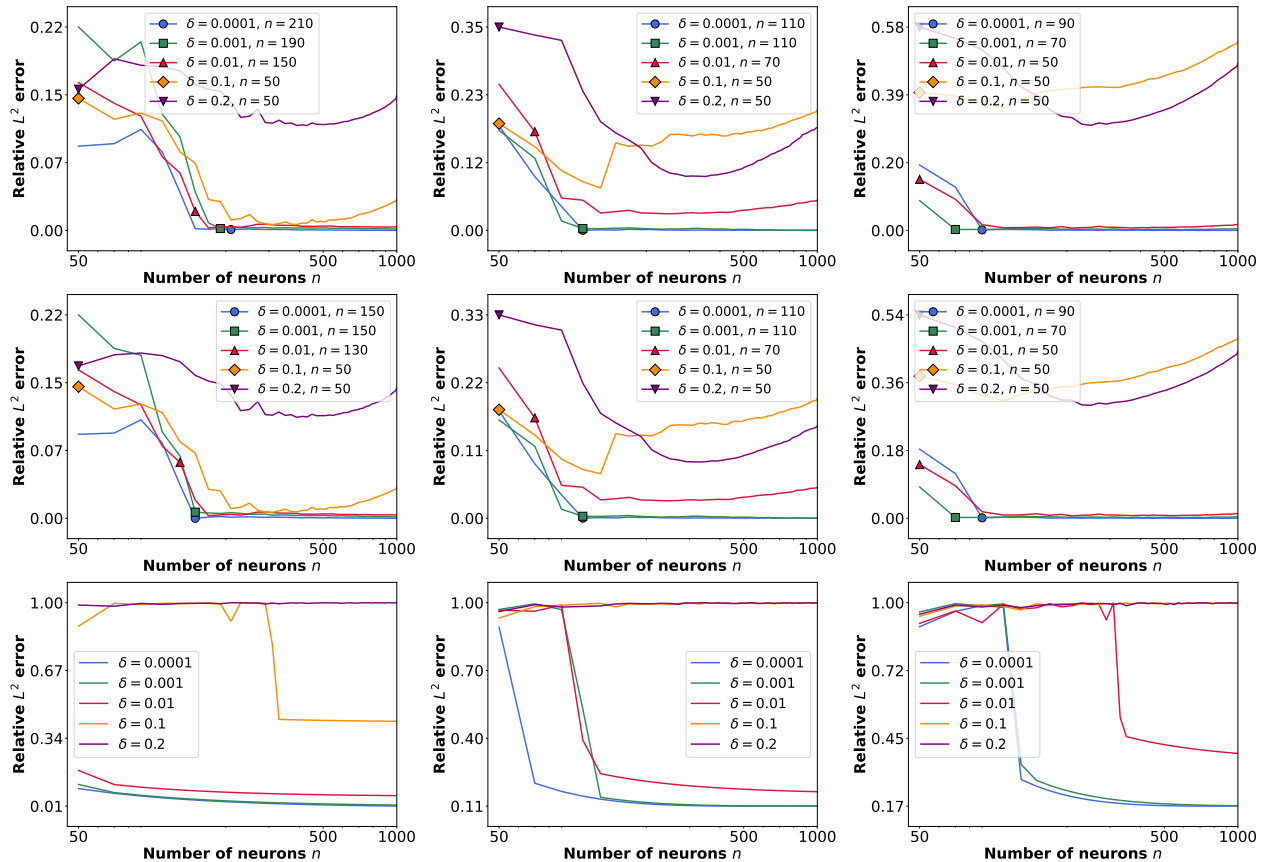


Fig. 2. Auto-convolution equation: Relative  $L^2$  error of  $f_n^\delta$  obtained by Algorithm 1 (top row), Algorithm 2 (middle row), and Tikhonov regularization (bottom row). Each column corresponds to a different random seed: 678, 765, 987 (from left to right). The marker on each curve highlights the first network architecture that satisfied the stopping criterion for each noise level, with  $\tau = 1.0001$ . The corresponding value of  $n$  (the stopping number) is indicated in the legend. In some figures, the blue circles ( $\delta = 0.0001$ ) and green squares ( $\delta = 0.001$ ) coincide.

By applying Alessandrini's identity in conjunction with standard energy estimates (cf. [57]), one obtains a local Lipschitz estimate – in fact, a global one within the uniformly elliptic  $L^\infty$  class – with respect to the  $L^\infty$ -norm. Specifically, there exist constants  $\gamma > 0$  and  $C = C(\gamma, \Omega)$  such that for any  $f$  satisfying  $\|f - f^\dagger\|_{L^\infty(\Omega)} < \gamma$ , the following inequality holds:

$$\|\Lambda_f - \Lambda_{f^\dagger}\|_{\mathcal{L}(H^{1/2}(\partial\Omega), H^{-1/2}(\partial\Omega))} \leq C \|f - f^\dagger\|_{L^\infty(\Omega)}.$$

We assume that the true conductivity  $f^\dagger$  and all admissible conductivities  $f$  belong to  $W^{1,\infty}(\Omega)$  and satisfy uniform ellipticity bounds  $0 < \alpha \leq f(x) \leq \beta$ . By Alessandrini's identity with elliptic regularity and Sobolev embeddings, one also obtains that there exist constants  $\gamma > 0$  and  $C = C(\gamma, \Omega)$  such that for any  $f$  satisfying  $\|f - f^\dagger\|_{H^1(\Omega)} < \gamma$

$$\|\Lambda_f - \Lambda_{f^\dagger}\|_{\mathcal{L}(H^{3/2}(\partial\Omega), H^{1/2}(\partial\Omega))} \leq C \|f - f^\dagger\|_{H^1(\Omega)},$$

which demonstrates that the forward map  $A$  is locally Lipschitz at  $f^\dagger$  with respect to the  $H^1(\Omega)$  norm.

In our numerical implementation, the forward problem is solved using finite difference method, while the inverse problem is solved by learning a mapping from the boundary data to the conductivity function. Moreover, instead of using a complete data  $\{(h, g) : g = \Lambda_f(h)\}$ , we only use a sample of data  $(h_1, g_1 = \Lambda_f(h_1))$  with

$$h_1(x, y) = \begin{cases} \sin(\pi x), & y = 0, \\ 0, & \text{otherwise.} \end{cases}$$

It is worth noting that, although a single measurement pair is sufficient for the current model problem, employing multiple sets of boundary measurements (e.g., 20 pairs derived from different voltage patterns) provides additional data and can lead to slightly improved reconstruction accuracy.

In the present example, the true conductivity is  $f^\dagger(x, y) = x + y + p_0$  with  $p_0 > 0$  on  $\Omega = [0, 1]^2$ , so  $f^\dagger$  is uniformly elliptic and essentially bounded:  $0 < p_0 \leq f^\dagger \leq p_0 + 2$ . Here,  $p_0$  is set to 1.

The numerical results for Examples 1-3 are reported in Figures 1, 2, and 3, respectively. These plots show how the relative  $L^2$  error of the neural network approximations produced by the three methods evolves with the number of neurons under different random seeds.

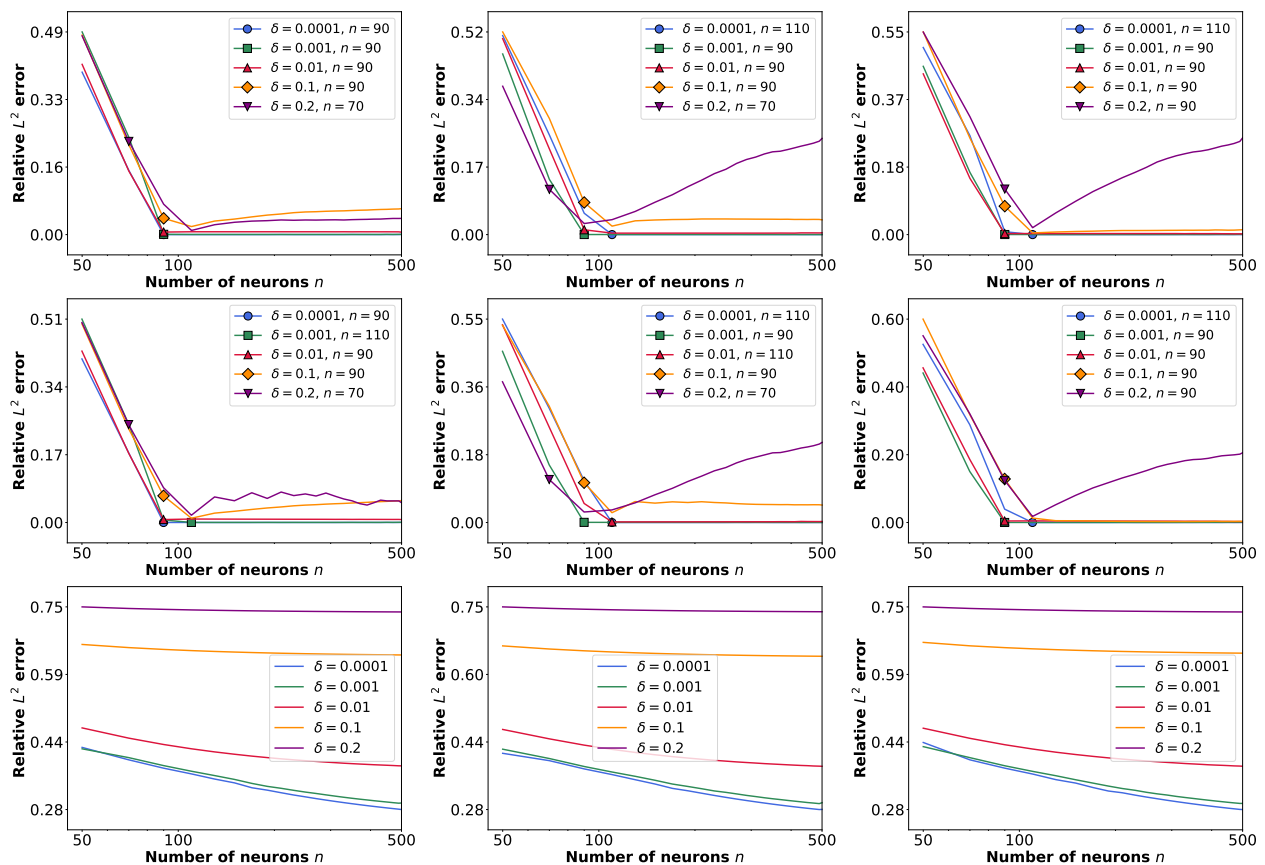


Fig. 3. EIT: Relative  $L^2$  error of  $f_n^\delta$  obtained by Algorithm 1 (top row), Algorithm 2 (middle row), and Tikhonov regularization (bottom row). Each column corresponds to a different random seed: 20, 30, 40 (from left to right). The marker on each curve highlights the first network architecture that satisfied the stopping criterion for each noise level, with  $\tau = 1.0001$ . The corresponding value of  $n$  (the stopping number) is indicated in the legend. In some figures, the blue circles ( $\delta = 0.0001$ ) and green squares ( $\delta = 0.001$ ) coincide.

To begin with, we draw attention to a phenomenon observed in Figure 1: in the first column, the solutions generated by Algorithms 1 and 2 display a pronounced blow-up behavior, namely, the relative error increases with the number of neurons  $n$  rather than decreasing. This effect reflects the intrinsic ill-posedness of the underlying inverse problem: as the network capacity grows, the approximation becomes increasingly sensitive to noise and numerical perturbations, which manifests as instability and error amplification. By contrast, Tikhonov regularization effectively suppresses this phenomenon. The improvement arises from the presence of the regularization term, which imposes an additional constraint that balances the fidelity to the data with the stability of the solution, thereby damping spurious oscillations and preventing uncontrolled error growth. This underscores the stabilizing effect of Tikhonov regularization, which provides a stronger balance between accuracy and stability than the alternative regularization strategies.

Beyond this specific behavior, more general trends can be identified across the results. From the second and third columns of Figure 1, and throughout Figures 2 and 3, it can be observed that, in general, the error of the neural network approximation decreases as the noise level  $\delta$  decreases and as the number of neurons  $n$  increases. However, for larger noise levels (e.g.,  $\delta = 0.1, 0.2$ ), the approximation error first decreases and then increases with growing  $n$ , resulting in an “L”-shaped curve. This observation suggests that, under high noise conditions, a simpler and smaller network architecture can already achieve satisfactory performance, while blindly increasing the network size does not necessarily improve the fitting accuracy and may instead lead to overfitting or degraded performance.

In addition, the points marked for the stopping index  $n$  of Algorithm 1 and Algorithm 2 indicate that both algorithms successfully terminate at finite iteration steps under all three random seed settings once the stopping criterion is met. For some high-noise cases, this threshold is relatively large, so the algorithm terminates earlier, even though the reconstruction error has not yet reached its minimum. This reflects the well-known semi-convergence effect: the discrepancy principle ensures stability rather than minimizing the true error, which explains why the stopping point can appear too early in noisy scenarios. Moreover, the specific values of the stopping  $n$  marked in the figures reflect that  $n = n(\delta)$  generally increases as  $\delta$  decreases, and are consistent with the theoretical estimate  $\mathcal{O}(1/\delta^2)$  provided in Theorems 1 and 2.

Regarding the Tikhonov regularization method, we examine the last row of the three figures. It can be observed that the error generally decreases initially and then stabilizes as the number of neurons increases when the noise level is small. In

some cases, the error continues to decrease without stabilizing, which may be attributed to the limitation of the maximum number of neurons ( $n_{\max}$ ) considered in the experiments. Moreover, for relatively large noise levels (e.g.,  $\delta = 0.1, 0.2$ ), the error is mainly dominated by the noise. Under such circumstances, as observed in some of the presented figures, increasing the number of neurons does not significantly reduce the approximation error, since the noise-induced instability persists regardless of model capacity. Overall, in the non-blow-up cases, Algorithms 1 and 2 as well as the Tikhonov regularization method are all capable of constructing neural network approximations with good accuracy. In comparison, Algorithms 1 and 2 tend to achieve approximations with smaller errors using relatively fewer neurons than the Tikhonov approach, whereas the Tikhonov method provides greater robustness and stability.

## VI. CONCLUSION AND OUTLOOK

In this work, we establish universal approximation theorems that account for both approximation error and measurement error in neural network-based regularization methods for general ill-posed problems. For iterative regularization, we develop the expanding neural network method and prove its regularization properties under different assumptions. As a by-product, we show that for data with high noise levels, a small network architecture is sufficient to obtain a good approximate solution. For variational regularization, we analyze neural network approximation within the framework of Tikhonov regularization. Under variational source conditions, we establish convergence rate results. In summary, this paper demonstrates that neural networks, when integrated with a slightly modified conventional regularization framework, can serve as effective regularization methods with theoretical guarantees. However, several challenges remain.

- Our theoretical analysis focuses on shallow (two-layer) neural networks in the classical Barron-space setting. Within this framework, we establish *the universal approximation theory of neural networks for inverse problems*: for a given noise level  $\delta$ , we proved that for the corresponding network width  $n = n(\delta)$ , the neural network approximation converges to the exact solution with certain convergence rates ( $\Phi(\tau\delta)$  under the variational source conditions). A current limitation is that the depth is fixed at  $l = 2$ , hence the approximation error scaling as  $\mathcal{O}(1/\sqrt{n})$  (Proposition 3), does not improve with increasing depth. Extending the analysis to networks with greater depth  $l$  is an important next step, with the goal of establishing convergence properties and rates when both  $n = n(\delta)$  and  $l = l(\delta)$  are adaptively chosen. However, a principal obstacle to extending our method to deep networks is that existing universal approximation theorems for DNNs rarely provide explicit, uniform bounds on network parameters (e.g., layerwise max-norm radii). Such bounds are needed so the algorithm searches within a radius-constrained network class where the feasible set  $X_{n,r}$  is compact, ensuring existence of minimizers and enabling convergence to the exact solution. Developing a general parameter-bounded DNN approximation theory is therefore key to achieving depth-adaptive rates.
- Beyond the ridge Barron models considered here, recent studies on graph convolutional neural networks (GCNNs) (e.g., [58]) have introduced shallow models of the form

$$f_M(\mathbf{x}, \Theta) = \frac{1}{M} \sum_{m=1}^M \mathbf{a}_m^\top \sigma(\mathbf{b}_m * \mathbf{x} + c_m), \quad \mathbf{x} \in \Omega.$$

Analogous to these neural networks, the corresponding function class is referred to as the *graph Barron space*  $\mathcal{B}_G$ . It has been shown to form a reproducing kernel Banach space, and in addition to satisfying a Lipschitz property, it enjoys a fundamental approximation theorem guaranteeing that any function in  $\mathcal{B}_G$  can be well-approximated by GCNN outputs. Incorporating this graph-convolutional extension into our framework represents a promising direction for future research.

- One particularly important open problem is the development of efficient optimization algorithms to solve the non-convex optimization problems (11), (12), and (13). Another key issue is the numerical implementation of the regularization stabilizer  $\mathcal{P}(f)$  in Tikhonov regularization (13). The current definition of  $\mathcal{P}(f)$  is derived from theoretical analysis, but it is nonlinear and difficult to implement using conventional optimization algorithms. Finding a suitable surrogate that meets both theoretical requirements and practical feasibility remains an intriguing and open challenge.

## APPENDIX A PROOF OF THEOREM 1

*Proof.* According to Lemma 1,  $X_{n,r(n)}$  is sequentially compact in  $L^2(\Omega)$ , hence compact. Since  $A$  is continuous from  $L^2(\Omega)$  to  $\mathcal{Y}$ , the functional  $J(f) = \|A(f) - g^\delta\|_{\mathcal{Y}}$  is continuous on  $X_{n,r(n)}$ . Therefore, by the Weierstrass theorem,  $J$  attains its minimum on  $X_{n,r(n)}$ .<sup>4</sup>

Note that  $r(n)$  is an increasing function with  $\lim_{n \rightarrow \infty} r(n) = B > c_\rho(f^\dagger)$ , there exists a constant  $N_1$  such that for all  $n \geq N_1$ :  $r(n) > c_\rho(f^\dagger)$ . Since  $A$  is continuous at  $f^\dagger$ , there exists a number  $\varepsilon_1 = \varepsilon_1(\delta)$  such that for all  $f$ :  $\|f - f^\dagger\|_{L^2(\Omega)} \leq \varepsilon_1$ :

$$\|A(f) - A(f^\dagger)\|_{\mathcal{Y}} \leq (\tau - 1)\delta.$$

<sup>4</sup>The minimizer may not be unique for a non-convex functional  $J(\cdot)$ .

Define  $N = N(\delta, f^\dagger, \Omega, d) = \max \left\{ N_1, \left( \frac{C(\Omega, d) \|f^\dagger\|_{\mathcal{B}_1}}{\varepsilon_1(\delta)} \right)^2, b(k_0) \right\}$ . Then, according to Proposition 3, for  $f^\dagger \in \mathcal{B}_1$  and any  $\delta > 0, n > N$ , there exists a two-layer network  $f_n \in X_{n, c_\rho(f^\dagger)} \subset X_{n, r(n)}$  such that

$$\|f^\dagger - f_n\|_{H^1(\Omega)} < \varepsilon_1(\delta).$$

Let  $k^* := \min\{k \in \mathbb{N}^+ | b(k) > N\}$ , hence  $k^* > k_0$  and  $b(k^* - 1) \leq N < b(k^*)$ . Now we show that  $n(\delta) \leq b(k^*), k(\delta) \leq k^*$ . Due to the Indeed, by the definition of  $f_{\bar{N}, k^*}$  in Algorithm 1 we have for  $\bar{N} = b(k^*) > N$ ,

$$\begin{aligned} J_{\bar{N}, k^*}^\delta &= \left\| A(f_{\bar{N}, k^*}^\delta) - g^\delta \right\|_{\mathcal{Y}} \leq \|A(f_{\bar{N}}) - g^\delta\|_{\mathcal{Y}} \\ &\leq \|A(f_{\bar{N}}) - A(f^\dagger)\|_{\mathcal{Y}} + \|A(f^\dagger) - g^\delta\|_{\mathcal{Y}} \leq (\tau - 1)\delta + \|g - g^\delta\|_{\mathcal{Y}} \leq \tau\delta, \end{aligned} \quad (26)$$

which gives that  $n(\delta) \leq \bar{N} = b(k^*)$  and  $k(\delta) \leq k^*$  by the definitions of  $n(\delta), k(\delta)$ .

Given that  $N(\delta) = \mathcal{O}((1/\varepsilon(\delta))^2)$  and the inequality  $k + 1 \leq b(k + 1) \leq C_b b(k)$  holds for all  $k \geq k_0$ , we observe that  $k^* - 1 \geq k_0$ . Consequently,

$$n(\delta) \leq b(k^*) \leq C_b b(k^* - 1) \leq C_b N = \mathcal{O}((1/\varepsilon(\delta))^2).$$

Moreover, since there exists a constant  $C > 0$  independent of  $\delta$  such that  $N(\delta) \leq C(1/\varepsilon(\delta))^2$  for all sufficiently small  $\delta$ , the monotonicity of  $b$  implies

$$k(\delta) \leq k^* \leq b^{-1}(C_b N(\delta)) \leq b^{-1}(C(1/\varepsilon(\delta))^2).$$

Therefore, the iteration process in Algorithm 1 terminates after at most  $k(\delta) = b^{-1}(C(1/\varepsilon(\delta))^2)$  steps, requiring at most  $n(\delta) = \mathcal{O}((1/\varepsilon(\delta))^2)$  neurons. Moreover, if the operator  $A$  is locally Hölder continuous of order  $\theta$  at  $f^\dagger$ , then for sufficient small  $\delta$ , we can take  $\varepsilon_1(\delta) = ((\tau - 1)/L_A \delta)^{1/\theta} < \gamma$ , which also yields (26). Hence,  $n(\delta) = \mathcal{O}(\delta^{-2/\theta})$ , and  $k(\delta) \leq b^{-1}(C\delta^{-2/\theta})$ .

Finally, let us prove the convergence of  $f_{n(\delta), k(\delta)}^\delta$  to the exact solution  $f^\dagger$  in  $H^1(\Omega)$  as  $\delta \rightarrow 0$  by contradiction. Assume that there exists a positive number  $\varepsilon$  and a sequence  $f_{n(\delta_k), k(\delta_k)}^{\delta_k}$  ( $\delta_k \searrow 0$ ) such that

$$\|f_{n(\delta_k), k(\delta_k)}^{\delta_k} - f^\dagger\|_{H^1(\Omega)} \geq \varepsilon > 0. \quad (27)$$

With a known estimation of  $\|f_{n(\delta), k(\delta)}^\delta\|_{\mathcal{B}_1} \leq r(n(\delta)) \leq B$ , we have that the  $\mathcal{B}_1$ -norm of the sequence  $\{f_{n(\delta), k(\delta)}^\delta\}$  generated by Algorithm 1 are uniformly bounded by a given constant  $B$ . Thus, by Lemma 2 there exists a convergent subsequence  $f_{n(\delta_{k_i}), k(\delta_{k_i})}^{\delta_{k_i}}$  such that  $f_{n(\delta_{k_i}), k(\delta_{k_i})}^{\delta_{k_i}} \rightarrow f^*$  in  $H^1(\Omega)$  as  $i \rightarrow \infty$ . Let  $\delta_{k_i} \rightarrow 0$  in the inequality (27), we obtain

$$\|f^* - f^\dagger\|_{H^1(\Omega)} \geq \varepsilon > 0. \quad (28)$$

On the other hand, by the definition of  $n(\delta_{k_i}), k(\delta_{k_i})$  in Algorithm 1, we have

$$0 \leq \left\| A(f_{n(\delta_{k_i}), k(\delta_{k_i})}^{\delta_{k_i}}) - g^{\delta_{k_i}} \right\|_{\mathcal{Y}} = J_{n(\delta_{k_i}), k(\delta_{k_i})}^{\delta_{k_i}}(f_{n(\delta_{k_i}), k(\delta_{k_i})}^{\delta_{k_i}}) \leq \tau\delta_{k_i}, \quad (29)$$

which implies that  $J_{n(\delta_{k_i}), k(\delta_{k_i})}^{\delta_{k_i}}(f_{n(\delta_{k_i}), k(\delta_{k_i})}^{\delta_{k_i}}) \rightarrow 0$  as  $\delta_{k_i} \rightarrow 0$ . Moreover, since  $f_{n(\delta_{k_i}), k(\delta_{k_i})}^{\delta_{k_i}} \rightarrow f^*$  and the functional  $\|A(\cdot) - g^\delta\|_{\mathcal{Y}}$  is continuous, we can deduce that  $\|A(f^*) - g\|_{\mathcal{Y}} = 0$ . Since  $A$  is injective, we have  $f^* = f^\dagger$ , which is a contradiction to (28).  $\square$

## APPENDIX B PROOF OF THEOREM 2

*Proof.* From Lemma 1 we know that  $X_{n, r(n)}$  is sequentially compact in  $L^2(\Omega)$ , and hence compact. Moreover,

$$J^1(f) := \|A(f) - g^\delta\|_{\mathcal{Y}} + \beta_n \mathcal{R}(f), \quad \beta_n = c_0 n^{-\frac{\theta}{2}},$$

is a continuous functional on  $X_{n, r(n)}$ . Therefore, by the Weierstrass theorem, there exists at least one minimizer  $f_n^\delta \in X_{n, r(n)}$  such that

$$J^1(f_n^\delta) = \min_{f \in X_{n, r(n)}} J^1(f).$$

Now, let us show that for any  $\delta > 0$  the iteration process in Algorithm 1 can be stopped at a finite step with finite neurons, that is,  $k(\delta) < +\infty, n(\delta) < +\infty$ . First, according to Proposition 3, for  $f^\dagger \in \mathcal{B}_1, \delta > 0$ , and

$$n > N_1 := \max \left\{ (C(\Omega, d) \|f^\dagger\|_{\mathcal{B}_1})^2 \cdot \left( \frac{3(L_A + L_{\mathcal{R}_1})}{(\tau - 1)\delta} \right)^{\frac{2}{\theta}}, \left( \frac{C(\Omega, d)}{\min\{\gamma_1, \gamma_2\}} \right)^2 \right\},$$

there exists a two-layer network  $f_n \in X_{n, c_\rho(f^\dagger)}$  with  $c_{\rho_n}(f_n) \leq c_\rho(f^\dagger)$  such that

$$\|f^\dagger - f_n\|_{H^1(\Omega)} < \min \left\{ \left( \frac{\tau - 1}{3(L_A + L_{\mathcal{R}_1})} \delta \right)^{\frac{1}{\theta}}, \gamma_1, \gamma_2 \right\}.$$

For the regularizer  $\mathcal{R} = \mathcal{R}_1$ , since the functional  $\mathcal{R}_1(\cdot)$  is  $L_{\mathcal{R}_1}$ -Lipschitz continuous at  $f^\dagger$ , if  $n \geq N_1$  we obtain that

$$|\mathcal{R}_1(f_n) - \mathcal{R}_1(f^\dagger)| \leq L_{\mathcal{R}_1} \frac{\tau - 1}{3(L_A + L_{\mathcal{R}_1})} \delta.$$

On the other hand, by the definition of  $r(n)$ , we have  $r(n) \rightarrow +\infty$ , hence for any  $\delta > 0$ , and all  $n \geq N_2$  with

$$N_2 = \max\{c_0^{\frac{2}{\theta}}, r^{-1}(c_\rho(f^\dagger)), b(k_0), \left(\frac{C(\Omega, d)}{\min\{\gamma_1, \gamma_2\}}\right)^2, \left(\frac{3\mathcal{R}_1(f^\dagger)}{(\tau - 1)\delta}\right)^{\frac{2}{\theta}}, \left(\frac{3c_\rho(f^\dagger)}{2(\tau - 1)\delta}\right)^{\frac{2}{\theta}}\},$$

where  $r^{-1}$  denotes the generalized inverse, i.e.,

$$r^{-1}(N) := \inf\{n \in \mathbb{N} : r(n) \geq N\}, \quad (30)$$

we have

$$r(n) \geq c_\rho(f^\dagger), \quad c_0 n^{-\frac{\theta}{2}} \mathcal{R}_1(f^\dagger) \leq \frac{\tau - 1}{3} \delta, \quad c_0 n^{-\frac{\theta}{2}} c_\rho(f^\dagger) \leq \frac{2(\tau - 1)}{3} \delta.$$

Without loss of generality, assume that  $\delta \leq \frac{3 \max\{\mathcal{R}_1(f^\dagger), c_\rho(f^\dagger)/2\}}{(\tau - 1)} \cdot \left(\max\left\{c_0^{\frac{2}{\theta}}, \left(\frac{C(\Omega, d)}{\min\{\gamma_1, \gamma_2\}}\right)^2, r^{-1}(c_\rho(f^\dagger)), b(k_0)\right\}\right)^{-\frac{2}{\theta}}$ .

In this case, we have  $N_2 = \max\left\{\left(\frac{3\mathcal{R}_1(f^\dagger)}{(\tau - 1)}\right)^{\frac{2}{\theta}} \delta^{-\frac{2}{\theta}}, \left(\frac{3c_\rho(f^\dagger)}{2(\tau - 1)}\right)^{\frac{2}{\theta}} \delta^{-\frac{2}{\theta}}\right\} \geq \max\{c_0^{\frac{2}{\theta}}, b(k_0)\}$ , and we denote:

$$N := N(\delta, f^\dagger, \Omega, d) = \max\{N_1, N_2\} = C_{\max} \cdot \delta^{-\frac{2}{\theta}} \geq \max\{c_0^{\frac{2}{\theta}}, b(k_0)\}, \quad (31)$$

where

$$C_{\max} := \max\left\{\left(\frac{3\mathcal{R}_1(f^\dagger)}{(\tau - 1)}\right)^{\frac{2}{\theta}}, \left(\frac{3c_\rho(f^\dagger)}{2(\tau - 1)}\right)^{\frac{2}{\theta}}, (C(\Omega, d) \|f^\dagger\|_{\mathcal{B}_1})^2 \cdot \left(\frac{3(L_A + L_{\mathcal{R}_1})}{(\tau - 1)}\right)^{\frac{2}{\theta}}\right\}. \quad (32)$$

According to the above discussion, for any  $\delta > 0$  and  $n \geq N$ , there exists a two-layer network  $f_n \in X_{n, c_\rho(f^\dagger)} \subset X_{n, r(n)}$  with  $\mathcal{R}_2(f_n) = c_{\rho_n}(f_n) \leq c_\rho(f^\dagger)$  such that

$$\|f^\dagger - f_n\|_{H^1(\Omega)} < \min\left\{\left(\frac{\tau - 1}{3(L_A + L_{\mathcal{R}_1})} \delta\right)^{\frac{1}{\theta}}, \gamma_1, \gamma_2\right\}, \quad c_0 n^{-\frac{\theta}{2}} \mathcal{R}_2(f_n) \leq c_0 n^{-\frac{\theta}{2}} c_\rho(f^\dagger) \leq \frac{2(\tau - 1)}{3} \delta, \quad (33)$$

and

$$\begin{aligned} c_0 n^{-\frac{\theta}{2}} \mathcal{R}_1(f_n) &\leq c_0 n^{-\frac{\theta}{2}} (|\mathcal{R}_1(f^\dagger)| + |\mathcal{R}_1(f_n) - \mathcal{R}_1(f^\dagger)|) \\ &\leq \frac{\tau - 1}{3} \delta + \left(c_0 L_{\mathcal{R}_1} \frac{\tau - 1}{3(L_A + L_{\mathcal{R}_1})}\right) n^{-\frac{\theta}{2}} \delta \leq \frac{2(\tau - 1)}{3} \delta. \end{aligned}$$

Denote  $k^* := \min\{k \in \mathbb{N}^+ | b(k) > N\}$ . Then, by definition,  $b(k^* - 1) \leq N < b(k^*)$  and  $k_0 < k^* \leq b^{-1}(N) + 1$ . Therefore, for  $\bar{N} = b(k^*) > N$ ,  $\mathcal{R} = \mathcal{R}_1$  or  $\mathcal{R} = \mathcal{R}_2$ . By the definition of  $f_{\bar{N}, k^*}^\delta$  in Algorithm 2, and the locally Hölder-type continuous property of  $A$  at  $f^\dagger$ , we have

$$\begin{aligned} J_{\bar{N}, k^*}^\delta &= \left\|A(f_{\bar{N}, k^*}^\delta) - g^\delta\right\|_{\mathcal{Y}} \leq \|A(f_{\bar{N}}) - g^\delta\|_{\mathcal{Y}} + c_0 n^{-\frac{\theta}{2}} \mathcal{R}(f_{\bar{N}}) \\ &\leq L_A \|f_{\bar{N}} - f^\dagger\|_{H^1(\Omega)}^\theta + \|A(f^\dagger) - g^\delta\|_{\mathcal{Y}} + c_0 n^{-\frac{\theta}{2}} \mathcal{R}(f_{\bar{N}}) \\ &\leq L_A \frac{\tau - 1}{3(L_A + L_{\mathcal{R}_1})} \delta + \|g - g^\delta\|_{\mathcal{Y}} + \frac{2(\tau - 1)}{3} \delta \leq \tau \delta. \end{aligned} \quad (34)$$

By the definition of the stopping indices  $n(\delta)$  and  $k(\delta)$  in the algorithm, this implies  $n(\delta) \leq \bar{N} = b(k^*)$  and  $k(\delta) \leq k^*$ . Combining these with the bound  $b(k^*) \leq C_b b(k^* - 1) \leq C_b N$ , and recalling that  $N = \mathcal{O}(\delta^{-2/\theta})$ , we finally obtain that,

$$n(\delta) = \mathcal{O}(\delta^{-2/\theta}), \quad \text{and} \quad k(\delta) \leq b^{-1}(C\delta^{-2/\theta}), \quad \text{as } \delta \rightarrow 0$$

for a sufficiently large constant  $C > 0$ .

Now, let us prove the convergence of  $f_{n(\delta), k(\delta)}^\delta$  to the exact solution  $f^\dagger$  as  $\delta \rightarrow 0$ . First, by Proposition 3, for any  $n(\delta)$ , there exists a two-layer network  $f_{n(\delta)} \in X_{n(\delta), c_\rho(f^\dagger)}$  such that

$$\|f^\dagger - f_{n(\delta)}\|_{H^1(\Omega)} \leq \frac{C(\Omega, d)}{\sqrt{n(\delta)}} \|f^\dagger\|_{\mathcal{B}_1}.$$

We first consider the case  $\mathcal{R} = \mathcal{R}_1$ . By the minimization property of  $f_{n(\delta_k),k(\delta_k)}^{\delta_k}$  and the property of  $\mathcal{R}_1(f) \geq C_{\mathcal{R}_1} \|f\|_{H^1(\Omega)}$ , similar to (34), we have

$$\begin{aligned} c_0 C_{\mathcal{R}_1} (n(\delta))^{-\frac{\theta}{2}} \|f_{n(\delta),k(\delta)}^\delta\|_{H^1(\Omega)} &\leq c_0 (n(\delta))^{-\frac{\theta}{2}} \mathcal{R}_1(f_{n(\delta),k(\delta)}^\delta) \\ &\leq \|A(f_{n(\delta)}) - g^\delta\|_{\mathcal{Y}} + c_0 (n(\delta))^{-\frac{\theta}{2}} \mathcal{R}_1(f_{n(\delta)}) \\ &\leq \|A(f_{n(\delta)}) - A(f^\dagger)\|_{\mathcal{Y}} + \|A(f^\dagger) - g^\delta\|_{\mathcal{Y}} + c_0 (n(\delta))^{-\frac{\theta}{2}} (|\mathcal{R}_1(f^\dagger)| + |\mathcal{R}_1(f_{n(\delta)}) - \mathcal{R}_1(f^\dagger)|) \\ &\leq \left( L_A(C(\Omega, d)\|f^\dagger\|_{\mathcal{B}_1})^\theta + c_0 |\mathcal{R}_1(f^\dagger)| + c_0 L_{\mathcal{R}_1}(C(\Omega, d)\|f^\dagger\|_{\mathcal{B}_1})^\theta \right) (n(\delta))^{-\frac{\theta}{2}} + \delta. \end{aligned}$$

Since  $n(\delta) \leq N$  with  $N$  defined in (31), it follows that  $\delta(n(\delta))^{\theta/2} \leq C_{\max}^{\theta/2}$ . Applying this bound, we obtain

$$\|f_{n(\delta),k(\delta)}^\delta\|_{H^1(\Omega)} \leq \frac{1}{c_0 C_{\mathcal{R}_1}} \left( (L_A + c_0 L_{\mathcal{R}_1})(C(\Omega, d)\|f^\dagger\|_{\mathcal{B}_1})^\theta + c_0 |\mathcal{R}_1(f^\dagger)| + C_{\max}^{\frac{\theta}{2}} \right),$$

hence  $\|f_{n(\delta),k(\delta)}^\delta\|_{H^1(\Omega)}$  are bounded by a constant independent of  $\delta$ . According to Lemma 2, there exists a convergent subsequence  $f_{n(\delta_k),k(\delta_k)}^{\delta_k}$  such that  $f_{n(\delta_k),k(\delta_k)}^{\delta_k} \rightarrow f^*$  in  $L^2(\Omega)$  as  $k \rightarrow \infty$ . Thus, similar to the proof of Theorem 1, approximate solutions  $f_{n(\delta),k(\delta)}^\delta$  converge to  $f^\dagger$  in  $L^2(\Omega)$  as  $\delta \rightarrow 0$ .

On the other hand, for  $\mathcal{R} = \mathcal{R}_2$ , since  $\mathcal{R}_2(f_{n(\delta)}) = c_{\rho_n}(f_{n(\delta)}) \leq c_\rho(f^\dagger)$ , we obtain

$$\begin{aligned} \|f_{n(\delta),k(\delta)}^\delta\|_{\mathcal{B}_1} &\leq c_{\rho_n}(f_{n(\delta),k(\delta)}^\delta) \leq \frac{1}{c_0} (n(\delta))^{\frac{\theta}{2}} \|A(f_{n(\delta)}) - g^\delta\|_{\mathcal{Y}} + \mathcal{R}_2(f_{n(\delta)}) \\ &\leq \frac{1}{c_0} (L_A(C(\Omega, d)\|f^\dagger\|_{\mathcal{B}_1})^\theta + \delta (n(\delta))^{\frac{\theta}{2}}) + c_{\rho_n}(f_{n(\delta)}) \\ &\leq \frac{1}{c_0} (L_A(C(\Omega, d)\|f^\dagger\|_{\mathcal{B}_1})^\theta + C_{\max}^{\frac{\theta}{2}}) + c_\rho(f^\dagger), \end{aligned}$$

this yields that  $\|f_{n(\delta),k(\delta)}^\delta\|_{\mathcal{B}_1}$  is bounded a constant independent of  $\delta$ . Hence, due to Lemma 2 and the above analysis, approximate solutions  $f_{n(\delta),k(\delta)}^\delta$  converge to  $f^\dagger$  in  $H^1(\Omega)$  as  $\delta \rightarrow 0$ .  $\square$

### APPENDIX C PROOF OF THEOREM 3

*Proof.* (a) Since  $\mathcal{T}_\alpha(f, g) \geq 0$  for all  $f \in X_{n,\infty}$ , the infimum

$$m_n := \inf_{f \in X_{n,\infty}} \mathcal{T}_\alpha(f, g)$$

is finite. Let  $\{f_{n,k}\}_{k \in \mathbb{N}} \subset X_{n,\infty}$  be a minimizing sequence, i.e.

$$\mathcal{T}_\alpha(f_{n,k}, g) \rightarrow m_n, \quad \text{as } k \rightarrow \infty.$$

Since  $m_n \leq \mathcal{T}_\alpha(0, g) = \mathcal{D}(A(0), g)$ , we may moreover assume that

$$\mathcal{T}_\alpha(f_{n,k}, g) \leq \mathcal{D}(A(0), g), \quad \text{for all } k \in \mathbb{N}.$$

It follows that, for all  $k$ ,

$$\varphi(c_{\rho_n}(f_{n,k})) = \mathcal{P}(f_{n,k}) \leq \mathcal{T}_\alpha(f_{n,k}, g) \leq \mathcal{D}(A(0), g).$$

Hence, by the monotonicity of  $\varphi$  and the definition of its generalized inverse  $\varphi^{-1}$  as in (30), we obtain

$$c_{\rho_n}(f_{n,k}) \leq \varphi^{-1}(\mathcal{D}(A(0), g)).$$

Recalling that  $\|b_j\|_1 + |c_j| = 1$  and  $c_{\rho_n}(f_{n,k}) = \frac{1}{n} \sum_{j=1}^n |a_j|$ , we obtain

$$|a_j| \leq n \cdot \frac{1}{n} \sum_{i=1}^n |a_i| = n c_{\rho_n}(f_{n,k}) \leq n \varphi^{-1}(\mathcal{D}(A(0), g)) =: R_n.$$

Thus  $f_{n,k} \in X_{n,R_n}$  for all  $k$ . For fixed  $R_n < \infty$ , the sequential compactness of  $X_{n,R_n}$  in  $L^2(\Omega)$ , provided by Lemma 1, implies that the sequence  $\{f_{n,k}\}$  admits a subsequence, denoted again by  $\{f_{n,k_\ell}\}$ , and some  $f_n^* \in X_{n,R_n}$  such that

$$f_{n,k_\ell} \rightarrow f_n^* \quad \text{in } L^2(\Omega).$$

By the lower semi-continuity of the functional  $\mathcal{T}_\alpha$ , ensured by Assumption 1, we obtain

$$\mathcal{T}_\alpha(f_n^*, g) \leq \liminf_{\ell \rightarrow \infty} \mathcal{T}_\alpha(f_{n,k_\ell}, g) = \inf_{f \in X_{n,\infty}} \mathcal{T}_\alpha(f, g),$$

and thus  $f_n^*$  is a minimizer of  $\mathcal{T}_\alpha(\cdot, g)$  on  $X_{n,\infty}$ .

(b) By the minimizing property of  $f_{n,k} \in \arg \min_{f \in X_{n,\infty}} \mathcal{T}_\alpha(f, g_k)$  and the properties of  $\mathcal{D}$  in Assumption 1, we have

$$\varphi(\|f_{n,k}\|_{\mathcal{B}_1}) = \mathcal{P}(f_{n,k}) \leq \mathcal{D}(A(f_{n,k}), g_k) + \mathcal{P}(f_{n,k}) = \mathcal{T}_\alpha(f_{n,k}, g_k) \leq \mathcal{T}_\alpha(0, g_k) = \mathcal{D}(A(0), g_k) \rightarrow \mathcal{D}(A(0), g),$$

as  $k \rightarrow \infty$ . Hence  $\{\mathcal{D}(A(0), g_k)\}_k$  is bounded, and by the monotonicity of  $\varphi$  and the definition of its generalized inverse, there exists  $R_n^1 < \infty$  such that

$$\|f_{n,k}\|_{\mathcal{B}_1} \leq R_n^1, \quad \text{for all } k,$$

i.e.  $\{f_{n,k}\} \subset X_{n,R_n^1}$ . By the sequential compactness of  $X_{n,R_n^1}$  in  $L^2(\Omega)$  (Lemma 1), there exists a subsequence, still denoted by  $\{f_{n,k_\ell}\}_{\ell=1}^\infty$ , and some  $f_n^* \in X_{n,R_n^1}$  such that

$$f_{n,k_\ell} \rightarrow f_n^* \quad \text{in } L^2(\Omega), \quad \text{as } \ell \rightarrow \infty.$$

Next we show that  $f_n^* \in \arg \min_{f \in X_{n,\infty}} \mathcal{T}_\alpha(f, g)$ .

By the lower semi-continuity of  $\mathcal{T}_\alpha$  with respect to  $f$ , and the continuity with respect to  $g$  (Assumption 1), together with  $f_{n,k_\ell} \rightarrow f_n^*$  and  $g_{k_\ell} \rightarrow g$  in  $\mathcal{Y}$ , we obtain

$$\mathcal{T}_\alpha(f_n^*, g) \leq \liminf_{\ell \rightarrow \infty} \mathcal{T}_\alpha(f_{n,k_\ell}, g_{k_\ell}).$$

On the other hand, by the minimizing property of  $f_{n,k_\ell}$  we have, for every  $f \in X_{n,\infty}$ ,

$$\mathcal{T}_\alpha(f_{n,k_\ell}, g_{k_\ell}) \leq \mathcal{T}_\alpha(f, g_{k_\ell}), \quad \text{for all } \ell,$$

and hence, using again the continuity of  $\mathcal{T}_\alpha$  with respect to  $g$ ,

$$\limsup_{\ell \rightarrow \infty} \mathcal{T}_\alpha(f_{n,k_\ell}, g_{k_\ell}) \leq \limsup_{\ell \rightarrow \infty} \mathcal{T}_\alpha(f, g_{k_\ell}) = \mathcal{T}_\alpha(f, g), \quad \forall f \in X_{n,\infty}.$$

Combining the last two inequalities yields

$$\mathcal{T}_\alpha(f_n^*, g) \leq \liminf_{\ell \rightarrow \infty} \mathcal{T}_\alpha(f_{n,k_\ell}, g_{k_\ell}) \leq \limsup_{\ell \rightarrow \infty} \mathcal{T}_\alpha(f_{n,k_\ell}, g_{k_\ell}) \leq \mathcal{T}_\alpha(f, g), \quad \forall f \in X_{n,\infty},$$

and therefore  $f_n^* \in \arg \min_{f \in X_{n,\infty}} \mathcal{T}_\alpha(f, g)$ .

(c) By (b), the family  $\{f_{n,k}\}_{k \in \mathbb{N}}$  is bounded in  $\mathcal{B}_1$  and hence relatively compact in  $L^2(\Omega)$ . Consequently, there exists a subsequence  $\{f_{n,k_\ell}\}_{\ell \in \mathbb{N}}$  and some  $f^\dagger \in \mathcal{B}_1$  such that

$$f_{n,k_\ell} \rightarrow f^\dagger \quad \text{in } L^2(\Omega), \quad \text{as } \ell \rightarrow \infty.$$

We now show that  $f^\dagger$  is an  $\mathcal{R}$ -minimizing solution of (1).

Let  $\bar{f} \in \mathcal{B}_1$  be an arbitrary solution of  $A(\bar{f}) = g$ . By the definition of the  $\mathcal{B}_1$ -norm:  $\|\bar{f}\|_{\mathcal{B}_1} = \inf_\rho c_\rho(\bar{f})$ , for any  $\varepsilon > 0$  there exists a representing probability  $\rho = \rho(\varepsilon)$  such that  $c_\rho(\bar{f}) \leq (1 + \varepsilon)\|\bar{f}\|_{\mathcal{B}_1}$ . Then, by Proposition 3 and the definition of the  $\mathcal{B}_p$ -norm in (5), for each  $n \in \mathbb{N}$ , there exists a two-layer network  $\bar{f}_n \in X_{n,\infty}$  such that

$$\|\bar{f}_n\|_{\mathcal{B}_1} \leq c_{\rho_n}(\bar{f}_n) \leq c_\rho(\bar{f}), \quad \|\bar{f} - \bar{f}_n\|_{H^1(\Omega)} \leq \frac{C(\Omega, d)}{\sqrt{n}} \|\bar{f}\|_{\mathcal{B}_1}. \quad (35)$$

By the monotonicity of  $\varphi$  we further obtain

$$\varphi(\|\bar{f}_n\|_{\mathcal{B}_1}) \leq \varphi(c_{\rho_n}(\bar{f}_n)) \leq \varphi(c_\rho(\bar{f})). \quad (36)$$

Using the minimizing property of  $f_{n,k_\ell} \in \arg \min_{f \in X_{n,\infty}} \mathcal{T}_\alpha(f, g_{k_\ell})$ , the condition  $\mathcal{D}(g, g^\delta) \leq \delta$ , and Assumption 1, we obtain

$$\begin{aligned} \mathcal{D}(A(f_{n,k_\ell}), g_{k_\ell}) + \alpha_{k_\ell, n} \varphi(c_{\rho_n}(f_{n,k_\ell})) & \\ & \leq \mathcal{D}(A(\bar{f}_n), g_{k_\ell}) + \alpha_{k_\ell, n} \varphi(c_{\rho_n}(\bar{f}_n)) \\ & \leq \mathcal{D}(A(\bar{f}_n), g_{k_\ell}) + \alpha_{k_\ell, n} \varphi(c_\rho(\bar{f})) \\ & \leq \tau \left( \mathcal{D}(A(\bar{f}_n), A(\bar{f})) + \mathcal{D}(g, g_{k_\ell}) \right) + \alpha_{k_\ell, n} \varphi(c_\rho(\bar{f})) \\ & \leq \tau \left( K_A \|\bar{f}_n - \bar{f}\|_{H^1(\Omega)}^s + \delta_{k_\ell} \right) + \alpha_{k_\ell, n} \varphi(c_\rho(\bar{f})), \end{aligned}$$

where we used (15) in the last step. Combining (35), (36) and the choice of  $\alpha_{k_\ell, n}$  in (16), we arrive at

$$\mathcal{D}(A(f_{n,k_\ell}), g_{k_\ell}) \leq \tau(Cn^{-s/2} + \delta_{k_\ell}) + \alpha_{k_\ell, n} \varphi(c_\rho(\bar{f})) \rightarrow 0, \quad \text{as } n, \ell \rightarrow \infty,$$

where  $C = K_A(C(\Omega, d)\|\bar{f}\|_{\mathcal{B}_1})^s$ . Moreover,

$$\varphi(\|f_{n,k_\ell}\|_{\mathcal{B}_1}) \leq \varphi(c_{\rho_n}(f_{n,k_\ell})) \leq \tau \alpha_{k_\ell, n}^{-1} (Cn^{-s/2} + \delta_{k_\ell}) + \varphi(c_\rho(\bar{f})) \rightarrow \varphi(c_\rho(\bar{f})), \quad \text{as } n, \ell \rightarrow \infty. \quad (37)$$

By the sequential lower semi-continuity of the data consistency functional  $\mathcal{D}$  (Assumption 1), we obtain

$$\mathcal{D}(A(f^\dagger), g) \leq \liminf_{n, \ell \rightarrow \infty} \mathcal{D}(A(f_{n, k_\ell}), g_{k_\ell}) \leq 0.$$

According to the non-negativity of  $\mathcal{D}$ , we have  $\mathcal{D}(A(f^\dagger), g) = 0$ , or equivalently  $A(f^\dagger) = g$ .

Finally, using the monotonicity of  $\varphi$  and the choice of probability  $\rho$ , and passing to the limit  $n, \ell \rightarrow \infty$  in (37), we obtain

$$\mathcal{R}(f^\dagger) = \varphi(\|f^\dagger\|_{\mathcal{B}_1}) \leq \varphi(c_\rho(\bar{f})) \leq \varphi((1 + \varepsilon)\|\bar{f}\|_{\mathcal{B}_1}).$$

Since  $\varepsilon > 0$  was arbitrary, letting  $\varepsilon \rightarrow 0$  yields  $\mathcal{R}(f^\dagger) \leq \mathcal{R}(\bar{f})$ . Thus  $f^\dagger$  is an  $\mathcal{R}$ -minimizing solution of  $A(f) = g$ .

In conclusion, along the subsequence  $\{f_{n, k_\ell}\}_{n, \ell}$  we have

$$f_{n, k_\ell} \rightarrow f^\dagger \quad \text{in } L^2(\Omega), \quad \text{as } n, \ell \rightarrow \infty$$

where  $f^\dagger$  is an  $\mathcal{R}$ -minimizing solution of (1). □

#### APPENDIX D PROOF OF THEOREM 4

*Proof.* Similar to the proof of Theorem 3(b), according to Proposition 3 and monotonicity of  $\varphi$ , for  $f^\dagger$  with its representing probability  $\rho$  obeying  $c_\rho(f^\dagger) \leq (1 + \varepsilon)\|f^\dagger\|_{\mathcal{B}_1}$ , there exists a two-layer network  $f_n^\dagger$  that satisfies

$$\varphi(\|f_n^\dagger\|_{\mathcal{B}_1}) \leq \varphi(c_{\rho_n}(f_n^\dagger)) \leq \varphi(c_\rho(f^\dagger)), \quad \|f^\dagger - f_n^\dagger\|_{H^1(\Omega)} \leq \frac{C(\Omega, d)}{\sqrt{n}} \|f^\dagger\|_{\mathcal{B}_1}. \quad (38)$$

Therefore, by the minimization property of  $f_{n, \alpha}^\delta$ , we obtain the estimate

$$\begin{aligned} \mathcal{D}(A(f_{n, \alpha}^\delta), g^\delta) + \alpha\varphi(c_{\rho_n}(f_{n, \alpha}^\delta)) &\leq \mathcal{D}(A(f_n^\dagger), g^\delta) + \alpha\varphi(c_{\rho_n}(f_n^\dagger)) \leq \mathcal{D}(A(f_n^\dagger), g^\delta) + \alpha\varphi(c_\rho(f^\dagger)) \\ &\leq \mathcal{D}(A(f_n^\dagger), g^\delta) + \alpha\varphi((1 + \varepsilon)\|f^\dagger\|_{\mathcal{B}_1}), \end{aligned}$$

by letting  $\varepsilon \rightarrow 0$  in the above equation, we have

$$\mathcal{D}(A(f_{n, \alpha}^\delta), g^\delta) + \alpha\varphi(\|f_{n, \alpha}^\delta\|_{\mathcal{B}_1}) \leq \mathcal{D}(A(f_n^\dagger), g^\delta) + \alpha\varphi(\|f^\dagger\|_{\mathcal{B}_1}). \quad (39)$$

Hence, it follows from (38),  $\mathcal{D}(g, g^\delta) \leq \delta$ , and the conditions of  $\mathcal{D}$  in Assumption 1 that

$$\begin{aligned} \|f_{n, \alpha}^\delta\|_{\mathcal{B}_1} &\leq \varphi^{-1}(\alpha^{-1}(\tau(\mathcal{D}(A(f_n^\dagger), A(f^\dagger)) + \mathcal{D}(g, g^\delta))) + \varphi(\|f^\dagger\|_{\mathcal{B}_1})) \\ &\leq \varphi^{-1}(\tau\alpha^{-1}(\delta + K_A(C(\Omega, d)\|f^\dagger\|_{\mathcal{B}_1})^s n^{-\frac{s}{2}}) + \varphi(\|f^\dagger\|_{\mathcal{B}_1})), \end{aligned}$$

this gives the estimate (20). Moreover, by noting that  $\mathcal{R}(f) = \varphi(\|f\|_{\mathcal{B}_1})$ , (39) also yields

$$\alpha(\mathcal{R}(f_{n, \alpha}^\delta) - \mathcal{R}(f^\dagger)) \leq \mathcal{D}(A(f_n^\dagger), g^\delta) - \mathcal{D}(A(f_{n, \alpha}^\delta), g^\delta), \quad (40)$$

According to Theorem 3(c), we have  $f_{n, \alpha}^\delta \rightarrow f^\dagger$  in  $L^2(\Omega)$  as  $\delta \rightarrow 0$  and  $n \rightarrow \infty$ , hence for every  $\varepsilon > 0$ ,  $\|f_{n, \alpha}^\delta - f^\dagger\|_{L^2(\Omega)} < \varepsilon$  holds for all sufficiently small  $\delta$  and sufficiently large  $n$ . By Assumption 2 and (40), we obtain

$$\begin{aligned} \alpha\mathcal{E}^\dagger(f_{n, \alpha}^\delta) &\leq \mathcal{D}(A(f_n^\dagger), g^\delta) - \mathcal{D}(A(f_{n, \alpha}^\delta), g) + \alpha\Phi(\mathcal{D}(A(f_{n, \alpha}^\delta), g)) \\ &\leq \tau(\mathcal{D}(A(f_n^\dagger), A(f^\dagger)) + \mathcal{D}(g, g^\delta)) - \mathcal{D}(A(f_{n, \alpha}^\delta), g^\delta) + \alpha\Phi(\tau(\mathcal{D}(A(f_{n, \alpha}^\delta), g^\delta) + \mathcal{D}(g, g^\delta))) \\ &\leq \tau(\mathcal{D}(A(f_n^\dagger), A(f^\dagger)) + \delta) - \mathcal{D}(A(f_{n, \alpha}^\delta), g^\delta) + \alpha\Phi(\tau\delta) + \alpha\Phi(\tau\mathcal{D}(A(f_{n, \alpha}^\delta), g^\delta)) \\ &\leq \tau(\delta + Cn^{-\frac{s}{2}}) + \alpha\Phi(\tau\delta) + \tau^{-1}\Phi^{-*}(\tau\alpha), \end{aligned}$$

where the last inequality holds due to the Young's inequality  $\alpha\Phi(\tau t) \leq t + \tau^{-1}\Phi^{-*}(\tau\alpha)$  for the inverse function  $\Phi^{-1}$  and its conjugate  $\Phi^{-*}$ .

Balancing  $\delta$  and  $n^{-s/2}$  yields  $n \asymp \delta^{-2/s}$  and a constant  $C_1 > 0$  with  $\delta + Cn^{-s/2} \leq C_1\delta$ . Then,

$$\mathcal{E}^\dagger(f_{n, \alpha}^\delta) \leq \Phi(\tau\delta) + \left(\tau C_1 \delta \alpha^{-1} + (\tau\alpha)^{-1} \Phi^{-*}(\tau\alpha)\right).$$

An a priori scale that balances the two terms in  $H_\delta := \left(\tau C_1 \delta \alpha^{-1} + (\tau\alpha)^{-1} \Phi^{-*}(\tau\alpha)\right)$  is

$$\alpha(\delta) \asymp \frac{\delta}{\Phi(\tau\delta)}. \quad (41)$$

Thus, for the choice  $n(\delta) \asymp \delta^{-2/s}$  and  $\alpha(\delta) \asymp \delta/\Phi(\tau\delta)$  we obtain

$$\mathcal{E}^\dagger(f_{n(\delta), \alpha(\delta)}^\delta) = \mathcal{O}(\Phi(\tau\delta)).$$

In the special case  $\Phi(t) = c_0 t^\mu$  with  $0 < \mu < 1$ , this reduces to  $\alpha(\delta) \asymp \delta^{1-\mu}$  and the rate  $\mathcal{E}^\dagger(f_{n(\delta), \alpha(\delta)}^\delta) = \mathcal{O}(\delta^\mu)$ . □

## REFERENCES

- [1] A. N. Tikhonov, A. V. Goncharky, V. V. Stepanov, and A. G. Yagola, *Numerical Methods for the Solution of Ill-Posed Problems*. Dordrecht, Netherlands: Kluwer Academic Publishers, 1995.
- [2] G. Cybenko, "Approximation by superpositions of a sigmoidal function," *Math. Control Signals Syst.*, vol. 2, no. 4, pp. 303–314, 1989.
- [3] K. Hornik, M. Stinchcombe, and H. White, "Multilayer feedforward networks are universal approximators," *Neural Netw.*, vol. 2, no. 5, pp. 359–366, 1989.
- [4] K. Hornik, "Approximation capabilities of multilayer feedforward networks," *Neural Netw.*, vol. 4, no. 2, pp. 251–257, 1991.
- [5] M. Stinchcombe and H. White, "Universal approximation using feedforward networks with non-sigmoid hidden layer activation functions," in *International 1989 Joint Conference on Neural Networks*. IEEE, 1989, pp. 613–617.
- [6] A. R. Barron, "Universal approximation bounds for superpositions of a sigmoidal function," *IEEE Trans. Inf. Theory*, vol. 39, no. 3, pp. 930–945, 1993.
- [7] M. Telgarsky, "Benefits of depth in neural networks," in *Conference on learning theory*. PMLR, 2016, pp. 1517–1539.
- [8] R. Eldan and O. Shamir, "The power of depth for feedforward neural networks," in *Conference on learning theory*. PMLR, 2016, pp. 907–940.
- [9] J. Lu, Z. Shen, H. Yang, and S. Zhang, "Deep network approximation for smooth functions," *SIAM J. Math. Anal.*, vol. 53, no. 5, pp. 5465–5506, 2021.
- [10] Z. Shen, H. Yang, and S. Zhang, "Optimal approximation rate of ReLU networks in terms of width and depth," *J. Math. Pures Appl.*, vol. 157, pp. 101–135, 2022.
- [11] Z. Shen, "Deep network approximation characterized by number of neurons," *Commun. Comput. Phys.*, vol. 28, no. 5, 2020.
- [12] S. Zhang, J. Lu, and H. Zhao, "Deep network approximation: Beyond RELU to diverse activation functions," *J. Mach. Learn. Res.*, vol. 25, no. 35, pp. 1–39, 2024.
- [13] C. Liu and M. Chen, "ReLU network with width  $d + \mathcal{O}(1)$  can achieve optimal approximation rate," in *International Conference on Machine Learning*, 2024.
- [14] D. Yarotsky and A. Zhevnerchuk, "The phase diagram of approximation rates for deep neural networks," in *Adv. Neural Inf. Process. Syst. (NeurIPS)*, vol. 33, 2020, pp. 13 005–13 015. [Online]. Available: <https://proceedings.neurips.cc/paper/2020/file/979a3f14bae523dc5101c52120c535e9-Paper.pdf>
- [15] S. Hon and H. Yang, "Simultaneous neural network approximation for smooth functions," *Neural Networks*, vol. 154, pp. 152–164, 2022.
- [16] W. E and B. Yu, "The deep Ritz method: a deep learning-based numerical algorithm for solving variational problems," *Commun. Math. Stat.*, vol. 6, no. 1, pp. 1–12, 2018.
- [17] J. Sirignano and K. Spiliopoulos, "DGM: A deep learning algorithm for solving partial differential equations," *J. Comput. Phys.*, vol. 375, pp. 1339–1364, 2018.
- [18] M. Raissi, P. Perdikaris, and G. E. Karniadakis, "Physics-informed neural networks: A deep learning framework for solving forward and inverse problems involving nonlinear partial differential equations," *J. Comput. Phys.*, vol. 378, pp. 686–707, 2019.
- [19] Y. Zang, G. Bao, X. Ye, and H. Zhou, "Weak adversarial networks for high-dimensional partial differential equations," *J. Comput. Phys.*, vol. 411, p. 109409, 2020.
- [20] A. Aggarwal, M. Mittal, and G. Battineni, "Generative adversarial network: An overview of theory and applications," *Int. J. Inf. Manag. Data Insights*, vol. 1, no. 1, p. 100004, 2021.
- [21] Z. Liu, Y. Wang, S. Vaidya, F. Ruehle, J. Halverson, M. Soljacic, T. Y. Hou, and M. Tegmark, "KAN: Kolmogorov–arnold networks," in *Proc. 13th Int. Conf. on Learning Representations (ICLR)*, 2025. [Online]. Available: <https://openreview.net/forum?id=Ozo7qJ5vZi>
- [22] A. Al-Arabi, A. Correia, G. Jardim, D. de Freitas Naiff, and Y. Saporito, "Extensions of the deep galerkin method," *Appl. Math. Comput.*, vol. 430, p. 127287, 2022.
- [23] J. N. Fuhg, A. Karmarkar, T. Kadeethum, H. Yoon, and N. Bouklas, "Deep convolutional ritz method: parametric PDE surrogates without labeled data," *Appl. Math. Mech.*, vol. 44, no. 7, pp. 1151–1174, 2023.
- [24] E. Haghighat, M. Raissi, A. Moure, H. Gomez, and R. Juanes, "A physics-informed deep learning framework for inversion and surrogate modeling in solid mechanics," *Comput. Methods Appl. Mech. Eng.*, vol. 379, p. 113741, 2021.
- [25] T. Kadeethum, D. O'Malley, J. N. Fuhg, Y. Choi, J. Lee, H. S. Viswanathan, and N. Bouklas, "A framework for data-driven solution and parameter estimation of pdes using conditional generative adversarial networks," *Nature Computational Science*, vol. 1, no. 12, pp. 819–829, 2021.
- [26] M. Raissi, A. Yazdani, and G. E. Karniadakis, "Hidden fluid mechanics: Learning velocity and pressure fields from flow visualizations," *Science*, vol. 367, no. 6481, pp. 1026–1030, 2020.
- [27] Y. Wang, J. Sun, J. Bai, C. Anitescu, M. S. Eshaghi, X. Zhuang, T. Rabczuk, and Y. Liu, "Kolmogorov–Arnold-Informed neural network: A physics-informed deep learning framework for solving forward and inverse problems based on Kolmogorov–Arnold Networks," *Comput. Methods Appl. Mech. Eng.*, vol. 433, p. 117518, 2025.
- [28] Y. LeCun, L. Bottou, Y. Bengio, and P. Haffner, "Gradient-based learning applied to document recognition," *Proc. IEEE*, vol. 86, no. 11, pp. 2278–2324, 1998.
- [29] O. Ronneberger, P. Fischer, and T. Brox, "U-net: Convolutional networks for biomedical image segmentation," in *Medical image computing and computer-assisted intervention—MICCAI 2015: 18th international conference, Munich, Germany, October 5–9, 2015, proceedings, part III 18*, 2015, pp. 234–241.
- [30] G. Bao, X. Ye, Y. Zang, and H. Zhou, "Numerical solution of inverse problems by weak adversarial networks," *Inverse Probl.*, vol. 36, no. 11, p. 115003, 2020.
- [31] S. Cen, B. Jin, K. Shin, and Z. Zhou, "Electrical impedance tomography with deep calderón method," *J. Comput. Phys.*, vol. 493, p. 112427, 2023.
- [32] Q. Wang, H. Zhang, X. Li, X. Duan, J. Wang, R. Zhang, H. Zhang, Y. Ma, H. Wang, and J. Jia, "Error-constraint deep learning scheme for electrical impedance tomography (EIT)," *IEEE Transactions on Instrumentation and Measurement*, vol. 71, pp. 1–11, 2021.
- [33] J. Adler and O. Öktem, "Solving ill-posed inverse problems using iterative deep neural networks," *Inverse Probl.*, vol. 33, no. 12, p. 124007, 2017.
- [34] R. Barbano, Ž. Kereta, A. Hauptmann, S. R. Arridge, and B. Jin, "Unsupervised knowledge-transfer for learned image reconstruction," *Inverse Probl.*, vol. 38, no. 10, p. 104004, 2022.
- [35] K. H. Jin, M. T. McCann, E. Froustey, and M. Unser, "Deep convolutional neural network for inverse problems in imaging," *IEEE Trans. Image Process.*, vol. 26, no. 9, pp. 4509–4522, 2017.
- [36] H. Li, J. Schwab, S. Antholzer, and M. Haltmeier, "NETT: Solving inverse problems with deep neural networks," *Inverse Probl.*, vol. 36, no. 6, p. 065005, 2020.
- [37] Z.-X. Cui, Q. Zhu, J. Cheng, B. Zhang, and D. Liang, "Deep unfolding as iterative regularization for imaging inverse problems," *Inverse Probl.*, vol. 40, no. 2, p. 025011, 2024.
- [38] K. Hammernik, T. Klatzer, E. Kobler, M. P. Recht, D. K. Sodickson, T. Pock, and F. Knoll, "Learning a variational network for reconstruction of accelerated MRI data," *Magn. Reson. Med.*, vol. 79, no. 6, pp. 3055–3071, 2018.
- [39] J. Schlemper, J. Caballero, J. V. Hajnal, A. N. Price, and D. Rueckert, "A deep cascade of convolutional neural networks for dynamic MR image reconstruction," *IEEE Trans. Med. Imaging*, vol. 37, no. 2, pp. 491–503, 2017.
- [40] H. W. Engl, M. Hanke, and A. Neubauer, *Regularization of inverse problems*. Springer Science & Business Media, 1996, vol. 375.
- [41] B. Kaltenbacher, A. Neubauer, and O. Scherzer, *Iterative Regularization Methods for Nonlinear Ill-Posed Problems*. Berlin, New York: Walter de Gruyter, 2008.
- [42] Y. Yagola, A. Leonov, and V. Titarenko, "Data errors and an error estimation for ill-posed problems," *Inverse Probl. Sci. Eng.*, vol. 10, no. 2, pp. 117–129, 2002.

- [43] K. Dorofeev and Y. Yagola, “The method of extending compacts and a posteriori error estimates for nonlinear ill-posed problems,” *J. Inverse Ill-Posed Probl.*, vol. 12, pp. 627–636, 2004.
- [44] Y. Zhang, R. Gong, M. Gulliksson, and X. Cheng, “A coupled complex boundary expanding compacts method for inverse source problems,” *J. Inverse Ill-Posed Probl.*, vol. 27, no. 1, pp. 67–86, 2019.
- [45] W. E. C. Ma, and L. Wu, “Barron spaces and the compositional function spaces for neural network models,” *arXiv preprint arXiv:1906.08039*, 2019.
- [46] Y. Li, S. Lu, P. Mathé, and S. V. Pereverzev, “Two-layer networks with the  $\text{ReLU}^k$  activation function: Barron spaces and derivative approximation,” *Numer. Math.*, vol. 156, no. 1, p. 319–344, Nov. 2023. [Online]. Available: <https://doi.org/10.1007/s00211-023-01384-6>
- [47] A. N. Tikhonov, L. A. S., and A. G. Yagola, *Nonlinear Ill-Posed Problems*. London, U.K.: Chapman and Hall: London, 1998.
- [48] P. Mathé, “Saturation of regularization methods for linear ill-posed problems in Hilbert spaces,” *SIAM J. Numer. Anal.*, vol. 42, pp. 968–973, 2006.
- [49] Y. Zhang and B. Hofmann, “On the second order asymptotical regularization of linear ill-posed inverse problems,” *Applicable Analysis*, vol. 99, pp. 1000–1025, 2020.
- [50] L. Yuan and Y. Zhang, “A scaling fractional asymptotical regularization method for linear inverse problems,” *Advances in Computational Mathematics*, vol. 51, no. 1, p. 1, 2025.
- [51] T. Hein and B. Hofmann, “Approximate source conditions for nonlinear ill-posed problems – chances and limitations,” *Inverse Probl.*, vol. 25, p. 035003, 2009.
- [52] B. Hofmann, B. Kaltenbacher, C. Poschl, and O. Scherzer, “A convergence rates result for Tikhonov regularization in Banach spaces with non-smooth operators,” *Inverse Probl.*, vol. 23, pp. 987–1010, 2007.
- [53] J. Flemming, *Variational Source Conditions Yield Convergence Rates*. Cham, Switzerland: Springer International Publishing, 2018, pp. 15–20.
- [54] Y. Deng, B. Hofmann, and F. Werner, “Deautoconvolution in the two-dimensional case,” *ETNA, Electron. Trans. Numer. Anal.*, vol. 59, pp. 24–42, 2023.
- [55] G. Fleischer, R. Gorenflo, and B. Hofmann, “On the autoconvolution equation and total variation constraints,” *Z. Angew. Math. Mech.*, vol. 79, no. 3, pp. 149–159, 1999.
- [56] K. Astala and L. Päivärinta, “Calderón’s inverse conductivity problem in the plane,” *Ann. Math.*, vol. 163, no. 1, pp. 265–299, 2006.
- [57] G. Alessandrini, “Singular solutions of elliptic equations and the determination of conductivity by boundary measurements,” *J. Differ. Equations*, vol. 84, no. 2, pp. 252–272, 1990.
- [58] S.-Y. Chung and Q. Sun, “Barron space for graph convolution neural networks,” *arXiv preprint arXiv:2311.02838*, 2023.